50272-101

REPORT DOCUMENTATION PAGE	1. REPORT NO. NSF/RA-780530	2.	3. Recipient's Accession No. PB292053
4. Title and Subtitle: Dynamic Response of a High Pressure Steam Pipe in a Fossil Fuel Power Plant			5. Report Date: April 1978 6.
7. Author(s): C.T. Sun. H. Lo, J.L. Bogdanoff, and Y.F. Chou			8. Performing Organization Rept. No.
9. Performing Organization Name and Address: Purdue University School of Aeronautics and Astronautics West Lafayette, Indiana 47907			10. Project/Task/Work Unit No. 11. Contract(C) or Grant(G) No. (C) (G) ENV7401575, GI41897
12. Sponsoring Organization Name and Address: Applied Science and Research Applications (ASRA) National Science Foundation 1800 G Street, N.W. Washington, D.C. 20550			13. Type of Report & Period Covered 14.

15. Supplementary Notes

16. Abstract (Limit: 200 words)

Piping systems in power plants are usually flexibly supported to allow thermal expansion. As a result, natural frequencies of the lower modes are low, and the systems are susceptible to damage due to dynamic disturbances such as earthquakes. The dynamic behavior of a high pressure steam pipe in the fossil fuel power plant of Unit #3 of the Tennessee Valley Authority at Paradise, Kentucky is investigated. This piping system connects the header at the top of the steam generator to the turbine at the ground level. The pipe is assumed fixed at the ground level and either fixed or attached to a shear beam model that represents the frame structure of the power plant. Free vibrations are first studied. Dynamic responses of the system subjected to the NS component of the ground acceleration in the El Centro 1940 earthquake record are obtained. The effects of damping, the material stiffness, and the frame structure on the piping responses are investigated.

17. Document Analysis a. Descriptors

Fossil-fuel power plants
Electric power plants
Steam pipes
High pressure tests
Dynamic response
Damping
Dynamic structural analysis
Earthquake resistant structures

b. Identifiers/Open-Ended Terms

c. COSATI Field/Group

18. Availability Statement: NTIS	19. Security Class (This Report)	21. No. of Pages: 54
	20. Security Class (This Page)	22. Price: PC A04/MF A01

(See ANSI-Z39.18) See Instructions on Reverse

OPTIONAL FORM 272 (4-77)
(Formerly NTIS-35)
Department of Commerce

ABSTRACT

The dynamic behavior of the high pressure steam pipe in the fossil fuel power plant of Unit #3 of TVA at Paradise, Kentucky is investigated. Both natural vibration and the dynamic response of the piping system subjected to a ground acceleration identical to the NS component of the ground acceleration in the El Centro 1940 earthquake are studied. In the analysis, the pipe is assumed to be fixed at both ends in one case; in the other case, the upper end of the pipe is connected to a shear beam that represents the boiler frame structure. The results are compared. The effects of damping and stiffness are also investigated.

INTRODUCTION

Piping systems in power plants are usually flexibly supported to allow thermal expansions. As a result, natural frequencies of the lower modes are low, and the systems are susceptible to damage due to dynamic disturbances such as earthquakes.

In the past, the dynamic analysis of piping systems was concentrated on simplifying the computational procedures [1-4]. With the aid of the finite element method, complicated piping systems can now be modeled almost exactly by finite elements, and the computation of natural frequencies, mode shapes as well as time history responses is no more a formidable job. The main difficulties that one encounters often lie in how to model correctly the supports of the piping system and the interaction of the system with the connected structures.

In this paper, we investigate the dynamic behavior of a high pressure steam pipe in the fossil fuel power plant of Unit #3 of TVA at Paradise, Kentucky. This piping system connects the header at the top of the steam generator to the turbine at the ground level. In this study, the pipe is assumed fixed at the ground level and either fixed or attached to a shear beam model that represents the frame structure of the power plant. Free vibrations are first studied. Dynamic responses of the system subjected to the NS component of the ground acceleration in the El Centro 1940 earthquake record are obtained. The effects of damping, the material stiffness, and the frame structure on the piping responses are investigated.

GEOMETRY AND ASSUMPTIONS

A sketch of the high pressure steam pipe is shown in Fig. 1. Except for the lower end portion, the pipe has 21.25 in. OD and 4 in. thickness. The central part runs vertically for about 175 ft. There are fifteen supports of which only one (the one closest to the upper end) provides lateral constraints. Except for Support A (see Fig. 1) which is supported by solid rods, all the others contain the counterpoise hangers, see Fig. 2. The counterpoise hanger allows additional displacements without increasing the load. In view of this, the support at Point A is modeled as an elastic axial member, while the others are regarded as having no restoring force during vibration. In other words, except for Support A, there is no vertical constraint at any other support. Since the lower modes of vibration contain mainly horizontal motions and vertical constraints at the supports can only elevate the frequencies for the vertical motions, the present assumptions seem to be quite reasonable from the design viewpoint.

The internal pressure in the system is 3800 psi. The material is A335P22, an iron base alloy with 2¼Cr - ½Mo. At operating temperature (1003°F) it has the following mechanical properties:

Modulus of Elasticity E: 23×10^6 psi

Tensile Strength : 53×10^3 psi

Yield Strength : 28×10^3 psi

For this investigation, both the elastic case and the case with 1.5 percent of the critical damping are considered. The effect of this amount of damping is obviously very small on the natural frequencies. Therefore, in the calculation of the natural frequencies, damping is neglected.

A pipe element provided by the finite element program SAPIV is used

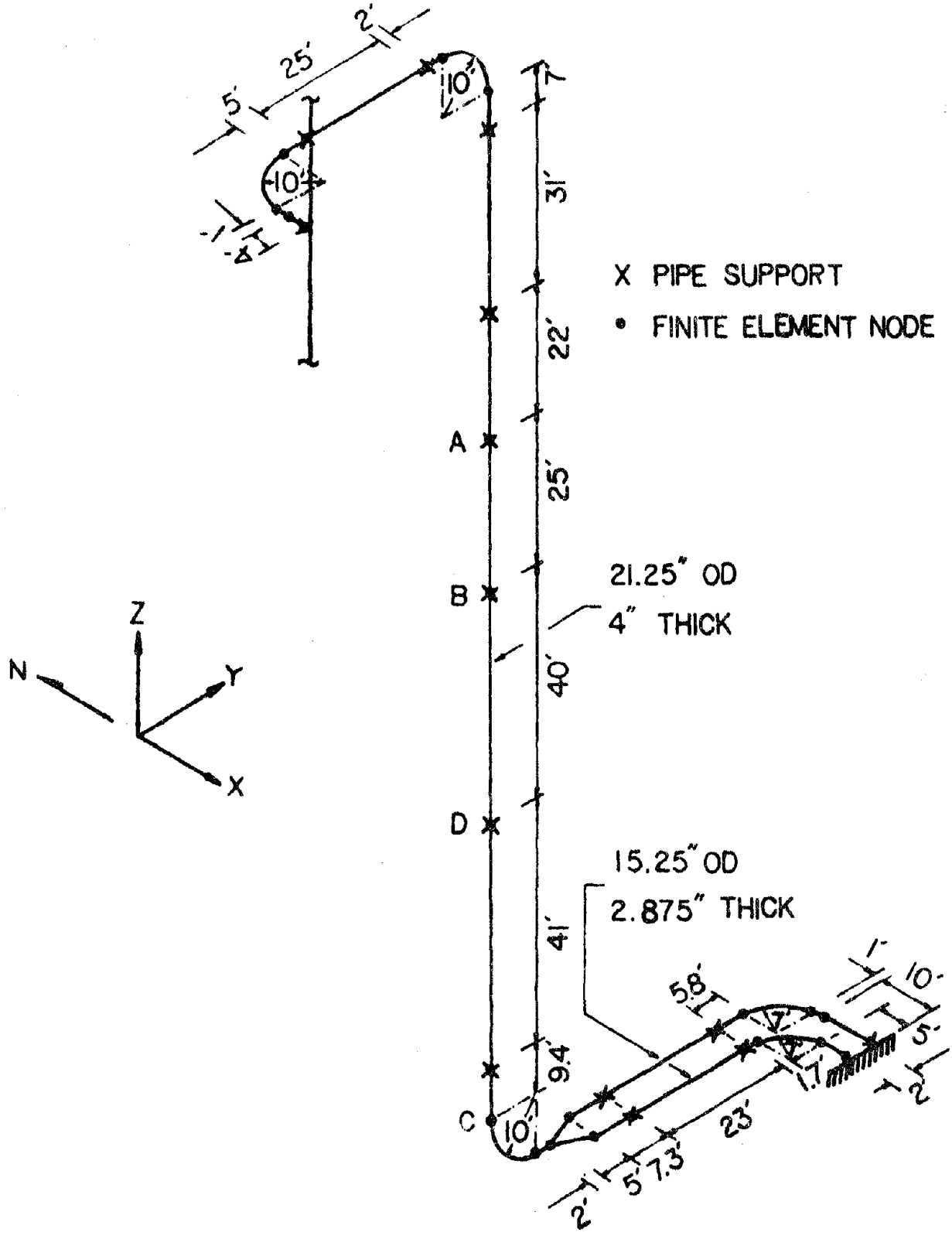

Fig. 1 Geometry of the piping system

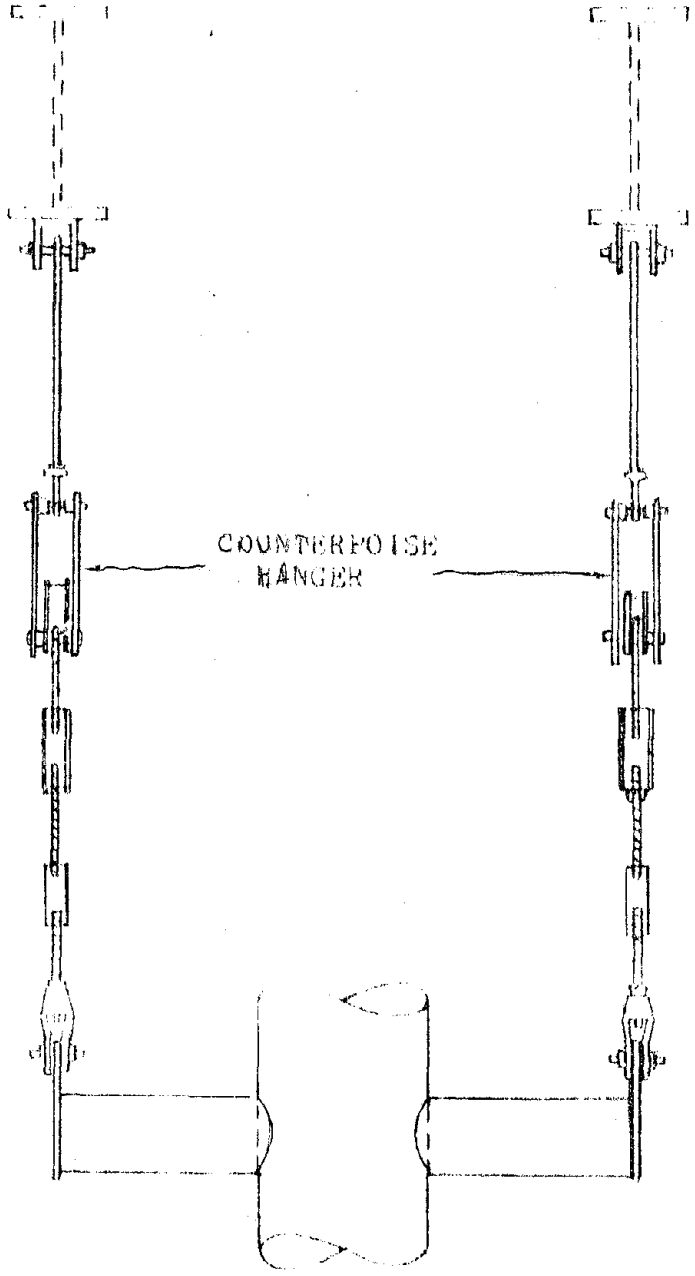

Fig. 2 Pipe support

for this study. The pipe element can be either straight or curved. Each element has two nodal points with six degrees of freedom at each node. Axial, bending, as well as torsional deformations are all accounted for.

Realistically, the piping system should be connected to the boiler and the supporting frame structure at the upper end. It is conceivable that analyzing the whole power plant structure in conjunction with the pipe is rather formidable. In this paper, we use a simple shear beam model developed by Chen, Sun, Bogdanoff and Lo [5] to represent the frame structure and the steam generator. The first two frequencies obtained from the simple model are 0.7352 Hz and 0.8392 Hz which are in good agreement with the results (0.7136 Hz and 0.8246 Hz) obtained by full scale finite element modeling [6]. It should be noted that it takes hours of computer time to compute one frequency with finite elements in contrast to a few seconds required by the simple model.

FREE VIBRATION

In the study of free vibration of the pipe, we consider two types of end conditions. First, we assume that both upper and lower ends are fixed. Second, the lower ends are assumed to be fixed while the upper end is assumed to be connected to a simple shear beam that represents the boiler frame structure; thus, the upper end is allowed to move in the x and y-directions as the shear beam.

Case 1: Fixed-Fixed System

In the numerical calculation, 29 elements (in general, one element between two supports except at the bends) are used for the pipe. The first ten frequencies are given in Table 1. The CP time for the computation is 47 seconds on CDC 6500.

The mode shapes for the lowest three modes are depicted in Fig. 3, 4, and 5, respectively. The first mode exhibits predominantly displacements in the x-direction; the second mode contains large x-direction motions with y-direction motion becoming more appreciable; in the third mode the y-direction motion is dominant. In Table 1, the last column summarizes the predominant direction for each of the first ten modes. Going through the first ten modes, we find that the motion in the z-direction is negligible for the first eight modes. The z-direction motion becomes substantial only in the ninth mode.

Case 2: Frame-Pipe System

The shear beam model for the boiler frame is connected to the pipe at the upper end as shown in Fig. 1. The lower ends are still assumed to be fixed.

The shear beam has distinct properties when deformed in the x-direction

MODE NO.	FREQUENCY HZ	PREDOMINANT DIRECTION
1	0.307	X
2	0.524	X
3	0.586	Y
4	0.996	X
5	1.606	Y
6	1.856	X
7	3.087	Y
8	3.390	X
9	3.858	Z
10	4.153	X

Table 1 Natural Frequencies for the fixed-fixed system

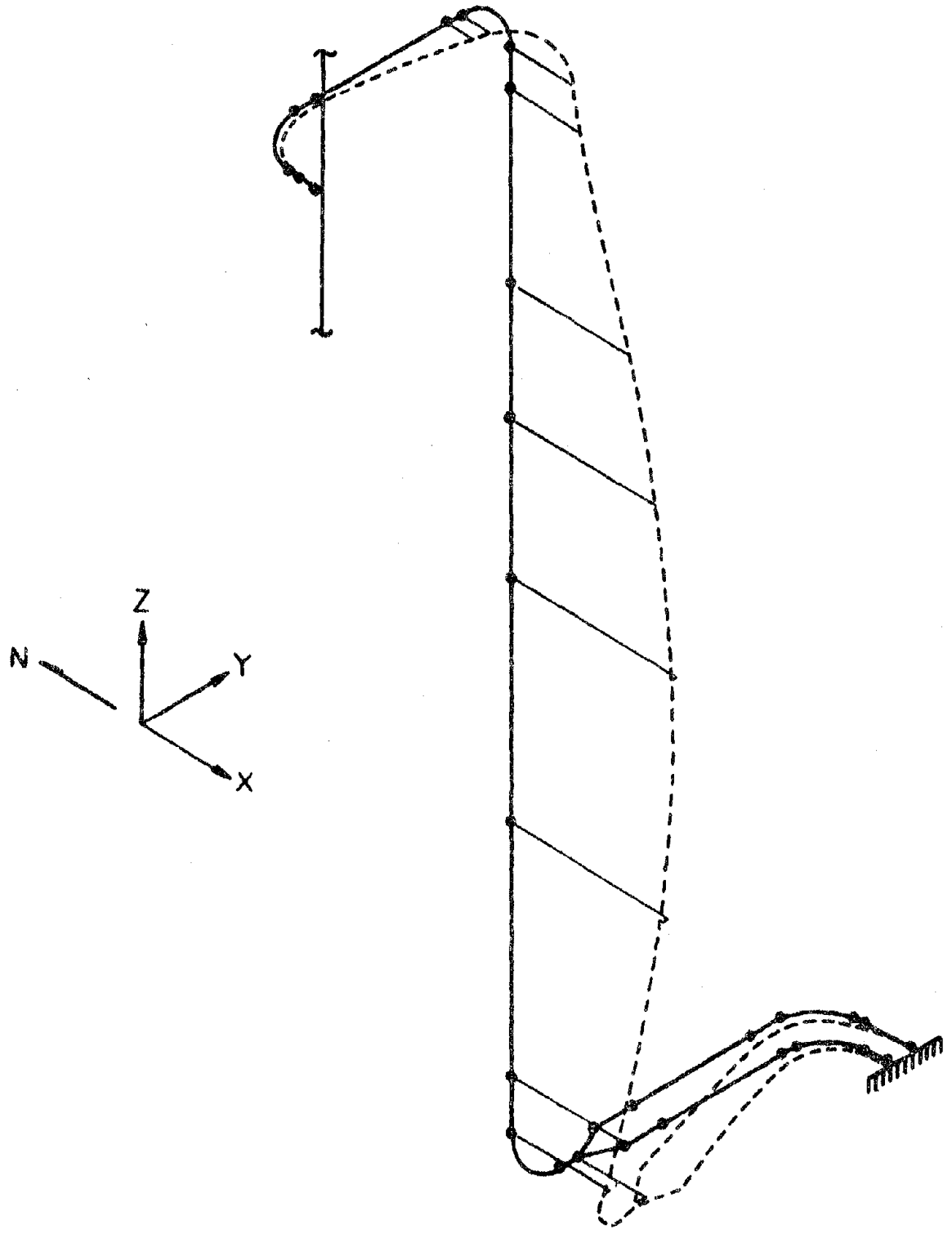

Fig. 3 First natural mode for the fixed-fixed system

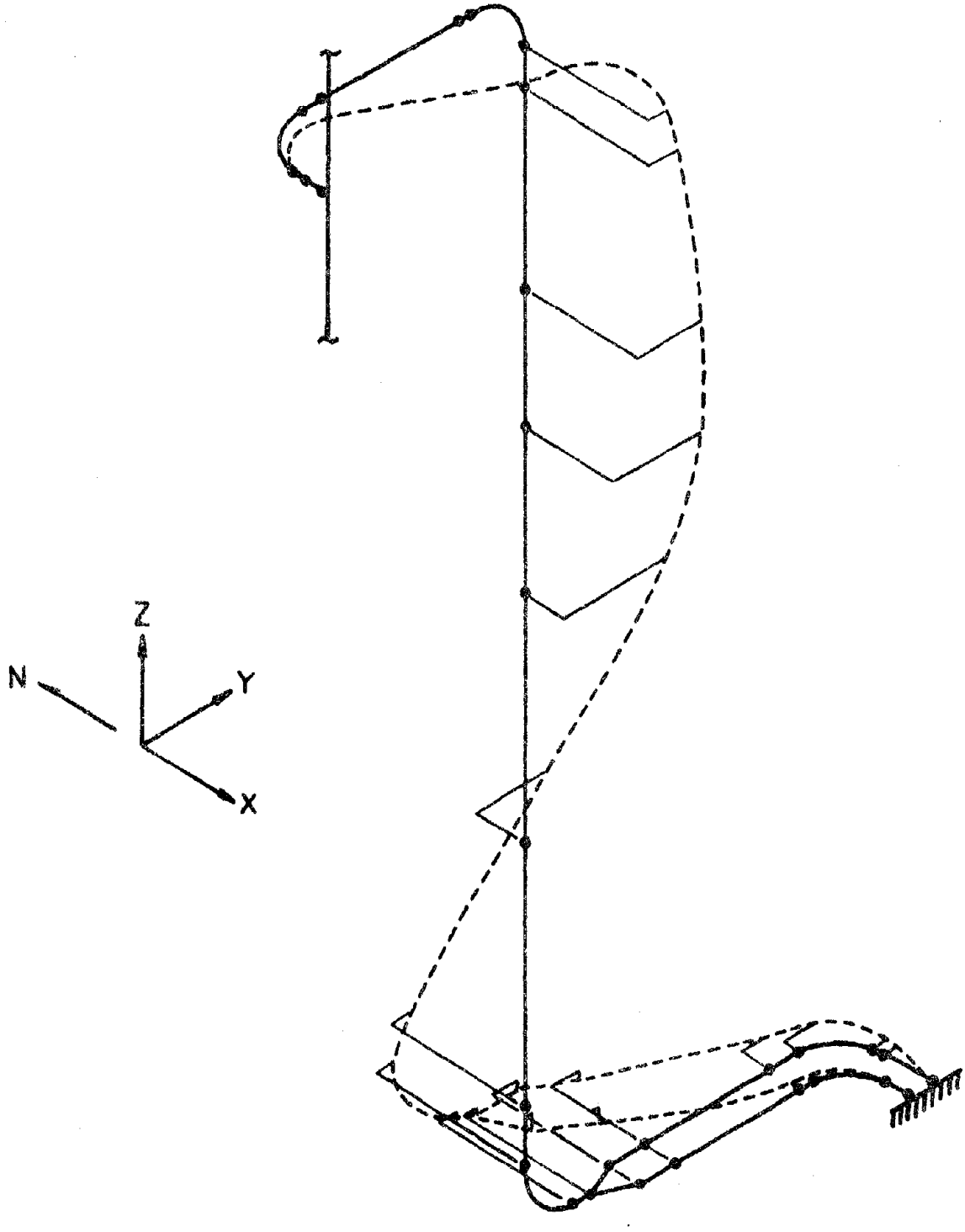

Fig. 4 Second natural mode for the fixed-fixed system

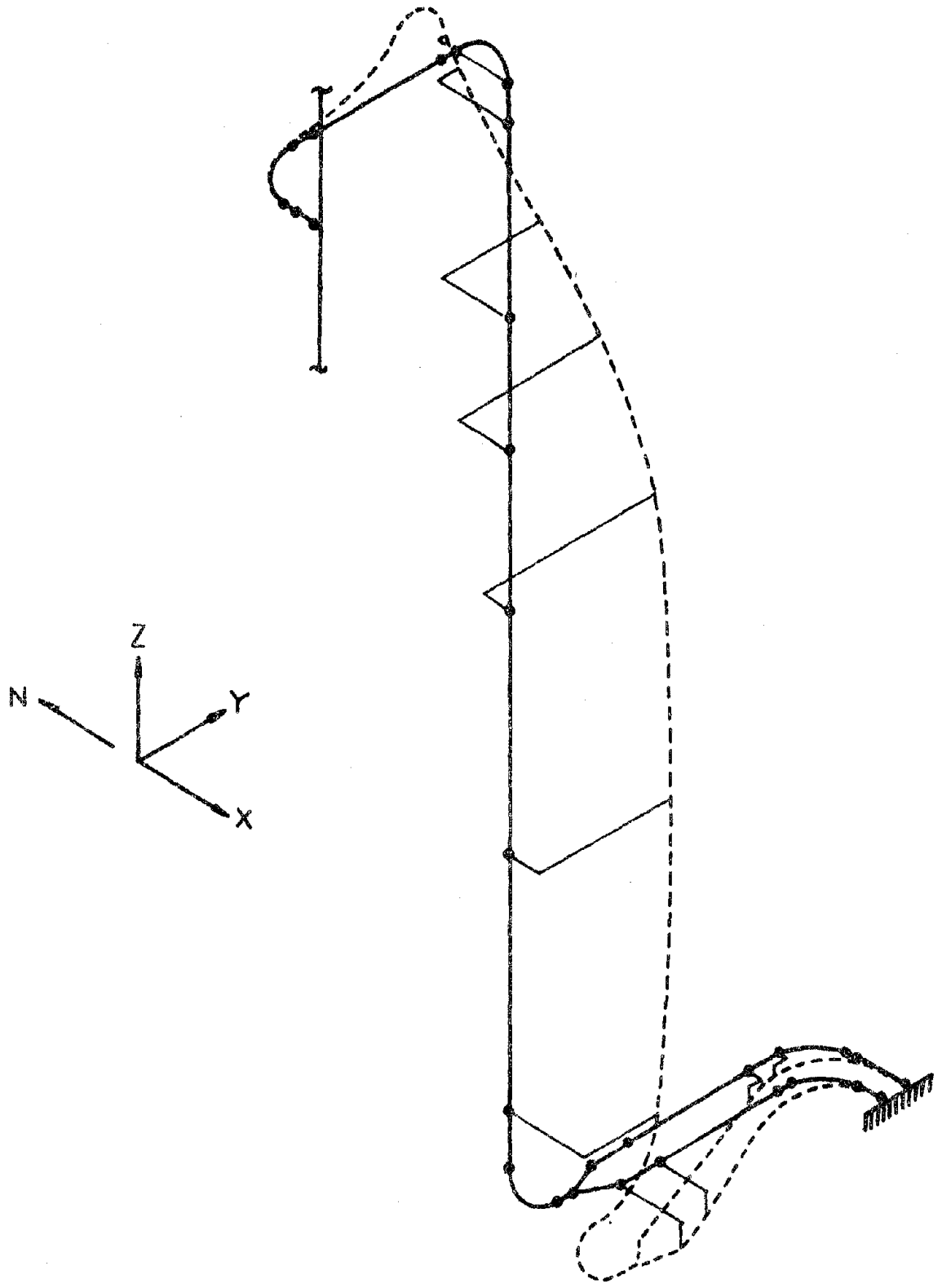

Fig. 5 Third natural mode for the fixed-fixed system

and y-direction independently. Mathematically, the equation of motion for the shear beam is identical to a truss member if the shear stiffness GA is replaced by the axial stiffness EA. In order to use the SAPIV program, the shear beam is replaced by two truss members placed horizontally parallel to the x-direction and the y-direction, respectively. Each truss member is modeled by 19 truss finite elements. Note that the axial displacements and axial forces in the truss members are interpreted as the transverse displacements and shear forces of the shear beam according to the analogy.

The first ten natural frequencies for the interactive frame-pipe system are given in Table 2. The first three mode shapes are almost identical to those for the fixed-fixed system. This similarity is also reflected by the fact that the natural frequencies for the first three modes are almost the same as the previous case. The mode shape for the fourth and fifth modes are shown in Figs. 6 and 7, respectively. It is seen that the amplitude of vibration of the frame structure is larger. It is noted that the natural frequencies for the fourth and fifth modes are very close to the first two natural frequencies of the shear beam that represents the boiler frame structure.

MODE NO.	FREQUENCY HZ	PREDOMINANT DIRECTION
1	0.307	X
2	0.523	X
3	0.585	Y
4	0.735	Y
5	0.837	X
6	0.996	X
7	1.606	Y
8	1.856	X
9	2.053	Y
10	2.585	X

Table 2 Natural frequencies for the frame-fixed system

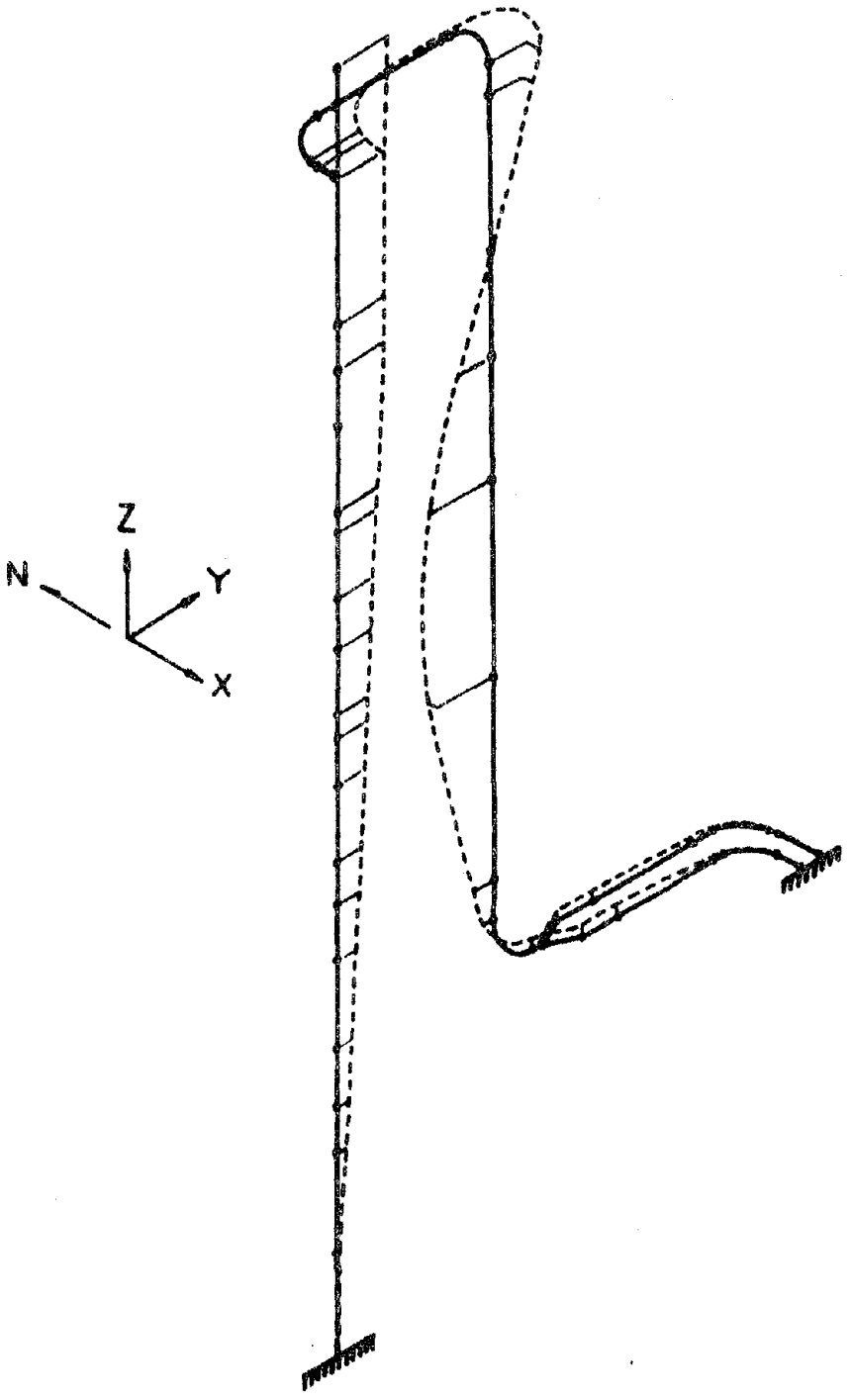

Fig. 6 Fourth natural mode for the frame-fixed system

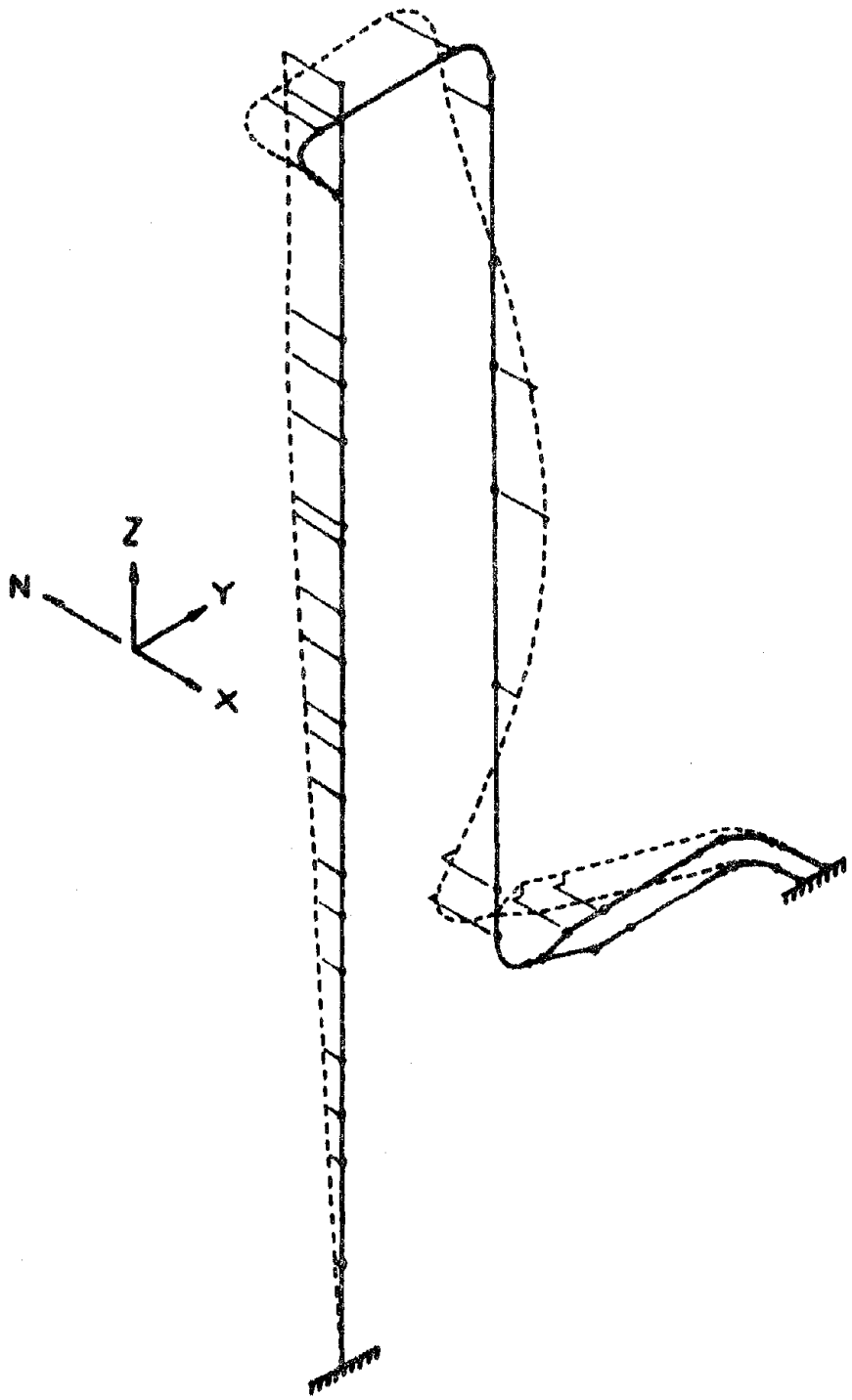

Fig.7 Fifth natural mode for the frame-fixed system

SEISMIC RESPONSE

The high pressure steam pipe is supported by the steel frame and connected to the steam generator and the turbine. During an earthquake, the piping system can pick up disturbances from the ground as well as from the boiler frame. It seems reasonable to neglect the interactions between the pipe and the frame through the hanger supports, since such supports transmit little lateral motions which have been found to be dominant in the dynamic response of the piping system. In this report, we assume that the seismic disturbance is transmitted to the lower ends of the pipe from the ground and to upper end through the interaction of the piping system and the boiler frame.

The NS component of the ground acceleration in the 1940 El Centro earthquake (see Fig. 8) is taken as the input for the ground accelerations in the x-, y- and z-directions. In other words, the three acceleration components are assumed identical.

The transient response of the piping system subjected to the earthquake motion is computed with 0, and 1.5 percent of critical damping. Two cases of boundary conditions are considered. In Case 1, it is assumed that the pipe is fixed at both upper and lower ends, and that, during the earthquake, the ground acceleration is applied to the lower ends only. In Case 2, the interaction of the pipe and the boiler frame is accounted for by using a simple shear beam model that represents the frame structure and the steam generator.

Under the ground acceleration $[\ddot{\delta}_g]$, the equations of motion are

$$[K][\delta_r] + [M][\ddot{\delta}_r] = -[M][\ddot{\delta}_g] \qquad (1)$$

where δ_r is the displacement of the structure relative to the ground.

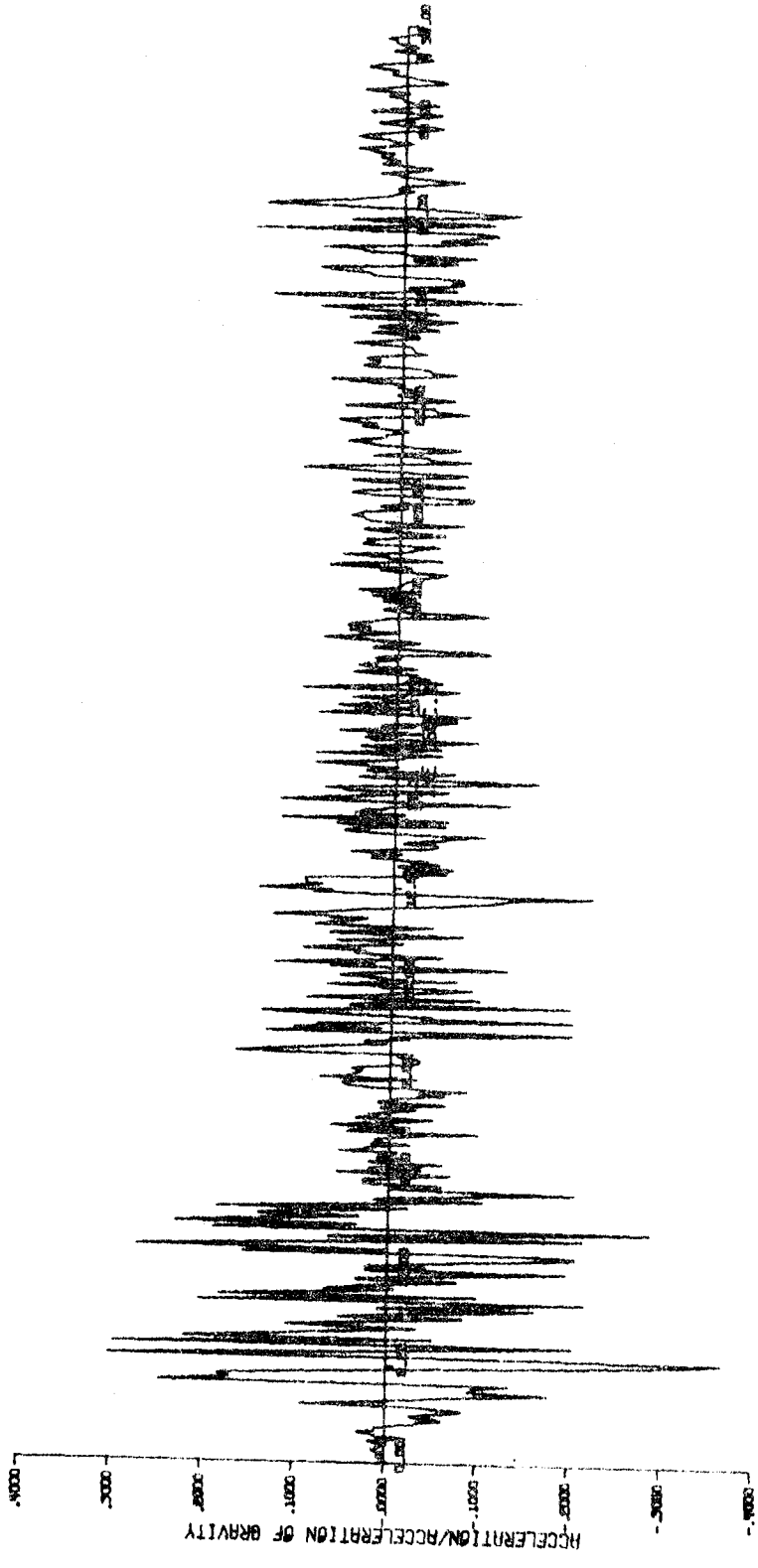

Fig. 8 The NS component of the ground acceleration in the 1940 El Centro Earthquake

Solution to Eq. (1) can be carried out either by direct integration or mode superpositions. The direct step-by-step integration is more effective for shock problems where many modes are included and fewer time steps are required. In the present study, by judging from the highly oscillatory nature and the long duration of the earthquake, the method of mode superposition is employed. The lowest ten vibration modes are used in the analysis.

The time-histories of the displacement in the x-direction at Point C for the two types of boundary conditions are presented in Figs. 9-12. Both 1.5 percent damping and purely elastic cases are considered. It can be seen that damping only affects the amplitude but not the period of vibration. However, the change of boundary condition from the fixed-fixed system to the frame-piping system does show a substantial difference in the response. Apparently, the flexibility of the frame structure adds to the motion of the piping system. As a result, the earthquake induced vibration is more severe if the pipe interacts with the frame.

Figure 13 shows the y-displacement at Point C for the fixed-fixed system. The corresponding result in the frame-fixed system is shown in Fig. 14. In both figures, the solid lines indicate the case of 1.5 percent damping while the dashed lines indicate the undamped case.

Figures 15 and 16 show the motions in the x- and y-directions, respectively, at the connection of the pipe and the boiler frame. In the undamped case, the maximum displacement in the x-direction reaches 14 in. which is twice larger than that of the damped response.

The maximum displacements in the x-direction at the nodal points (the pipe supports, in general) and the corresponding times of occurence for the fixed-fixed system and the frame-fixed system are presented in Figs. 17 and

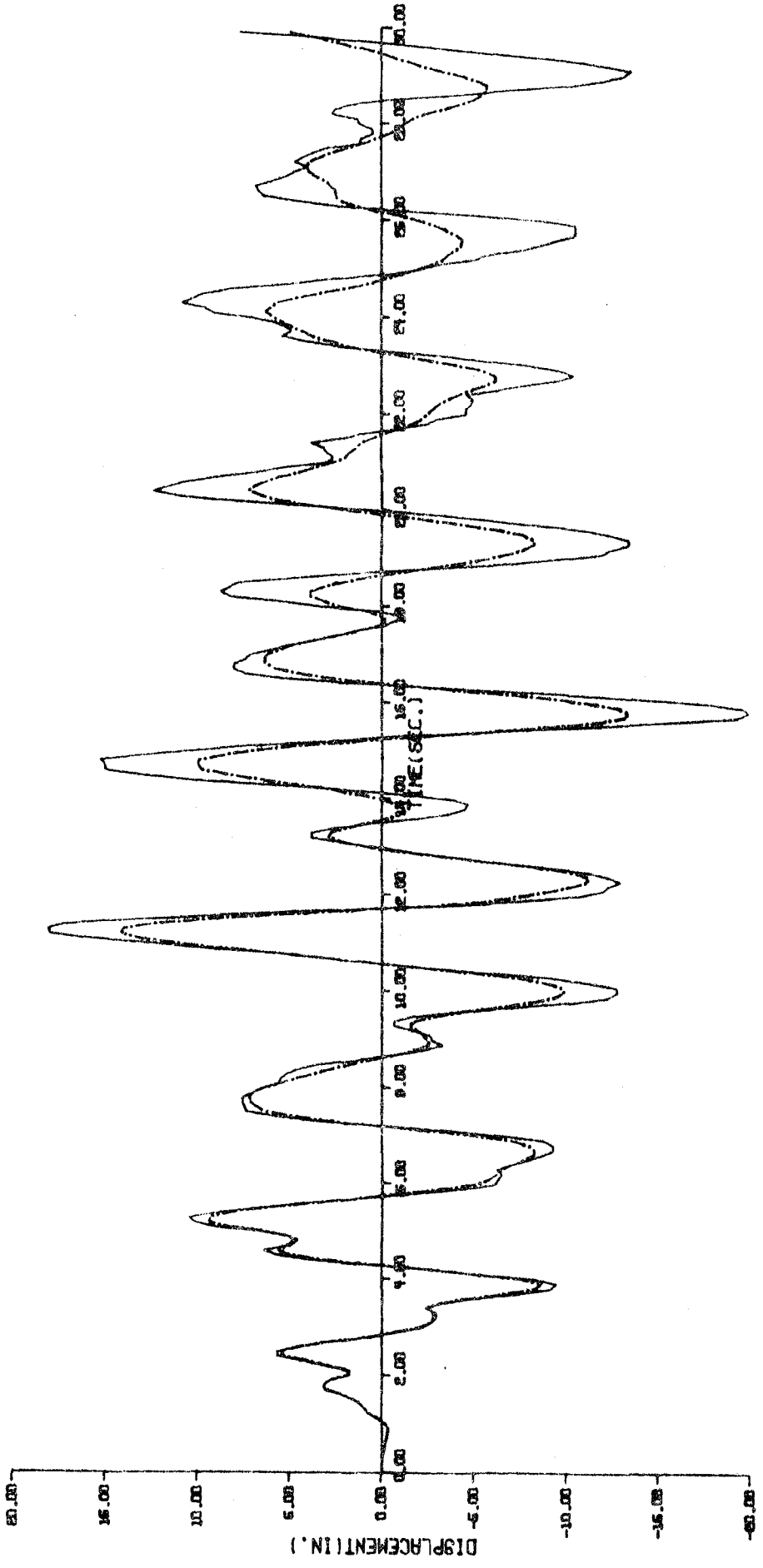

Fig. 9 Time history of the x-displacement at Point C for the fixed-fixed case.
_____ undamped; _____ . _____ 1.5% damping.

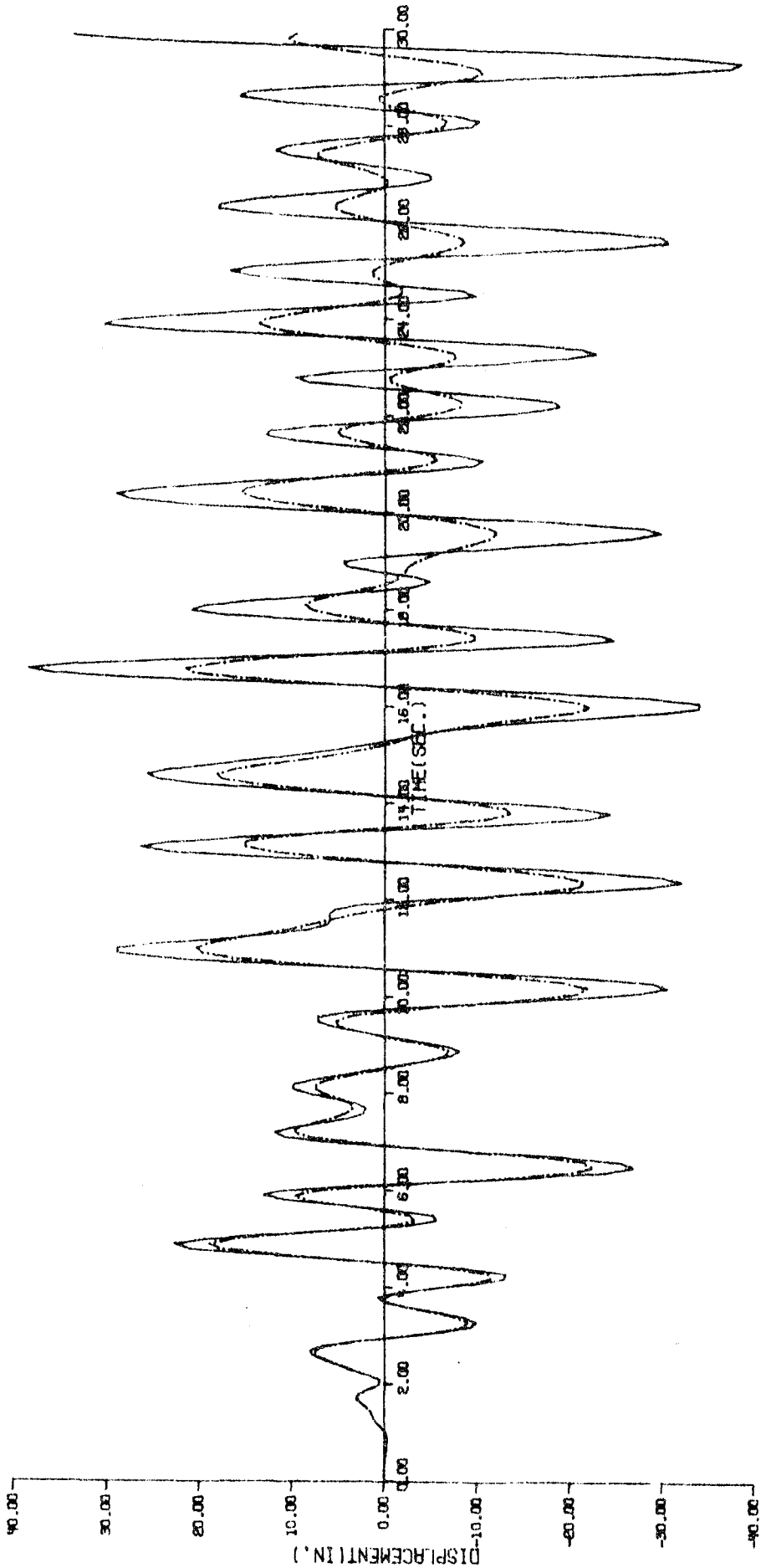

Fig. 10 Time history of the x-displacement at Point C for the frame-fixed case.
undamped; ——— . ——— . 1.5% damping.

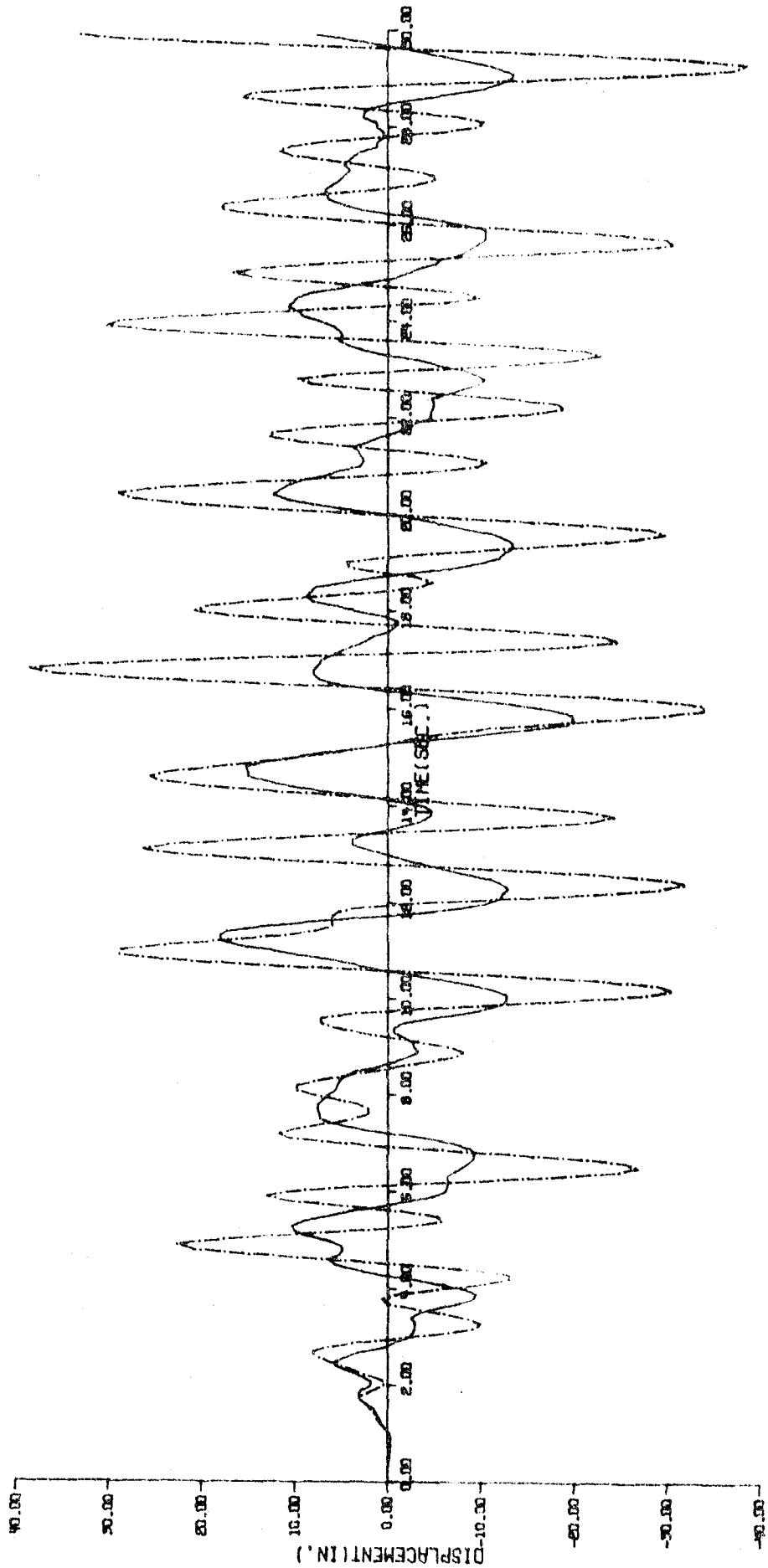

Fig. 11 Comparison of time histories of the x-displacement at Point C with 0 damping.
___ fixed-fixed case; ___ . ___ . frame-fixed case.

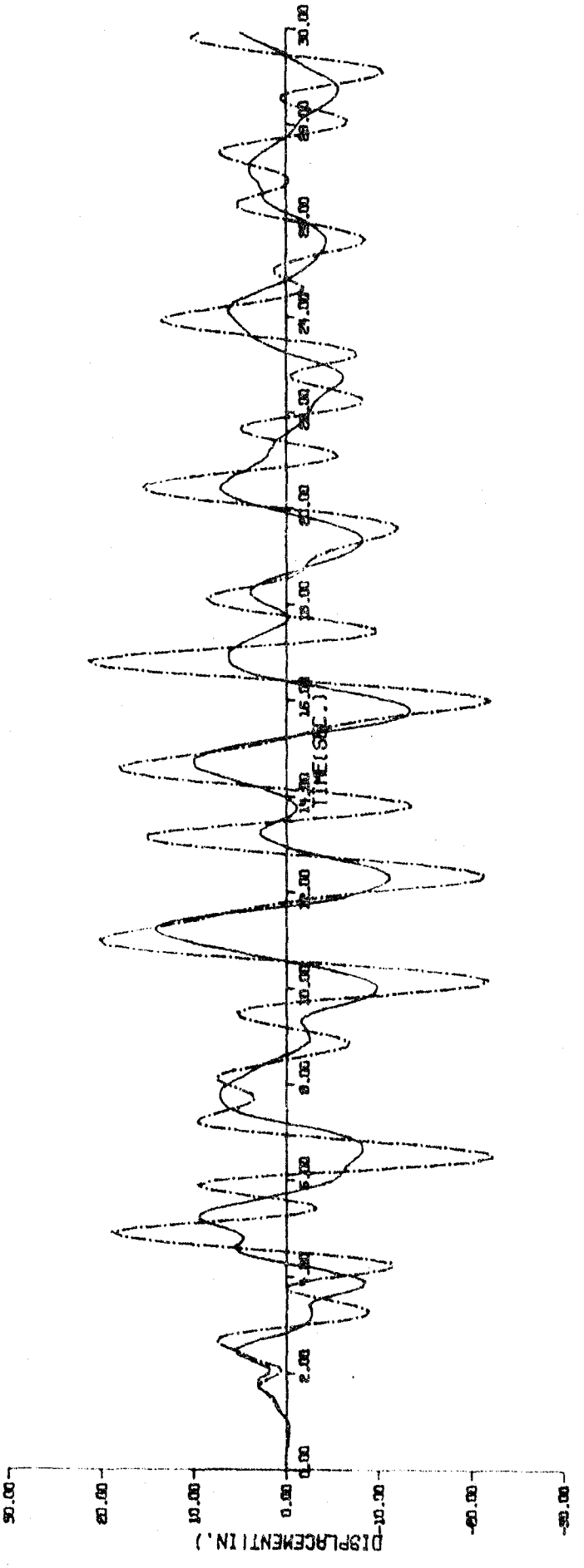

Fig. 12 Comparison of time histories of the x-displacement at Point C with 1.5% damping. ____ fixed-fixed case; ___ . ___ . frame-fixed case.

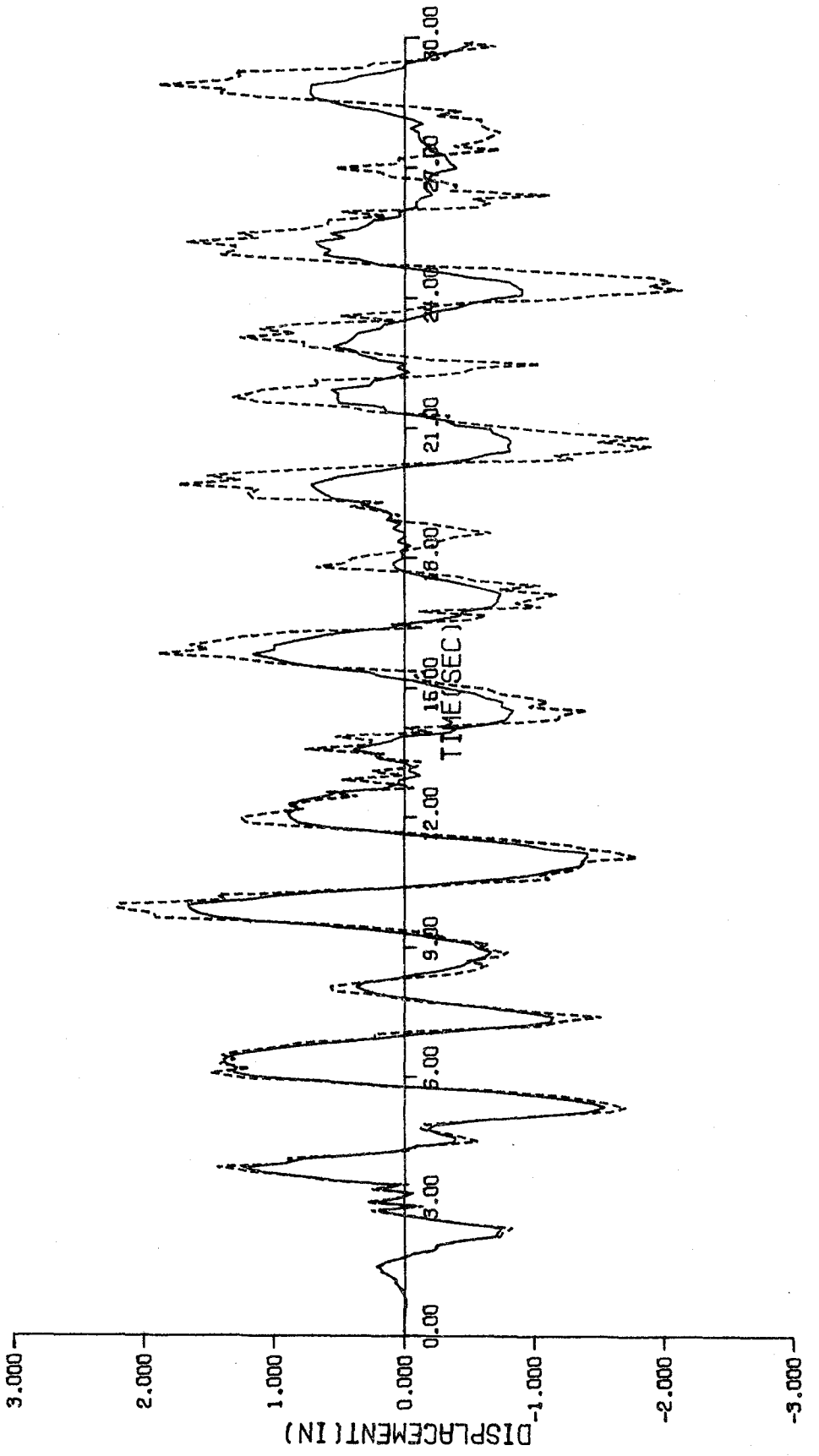

Fig. 13 Time history of the y-displacement at Point C for the fixed-fixed case.
---- undamped; ____ 1.5% damping.

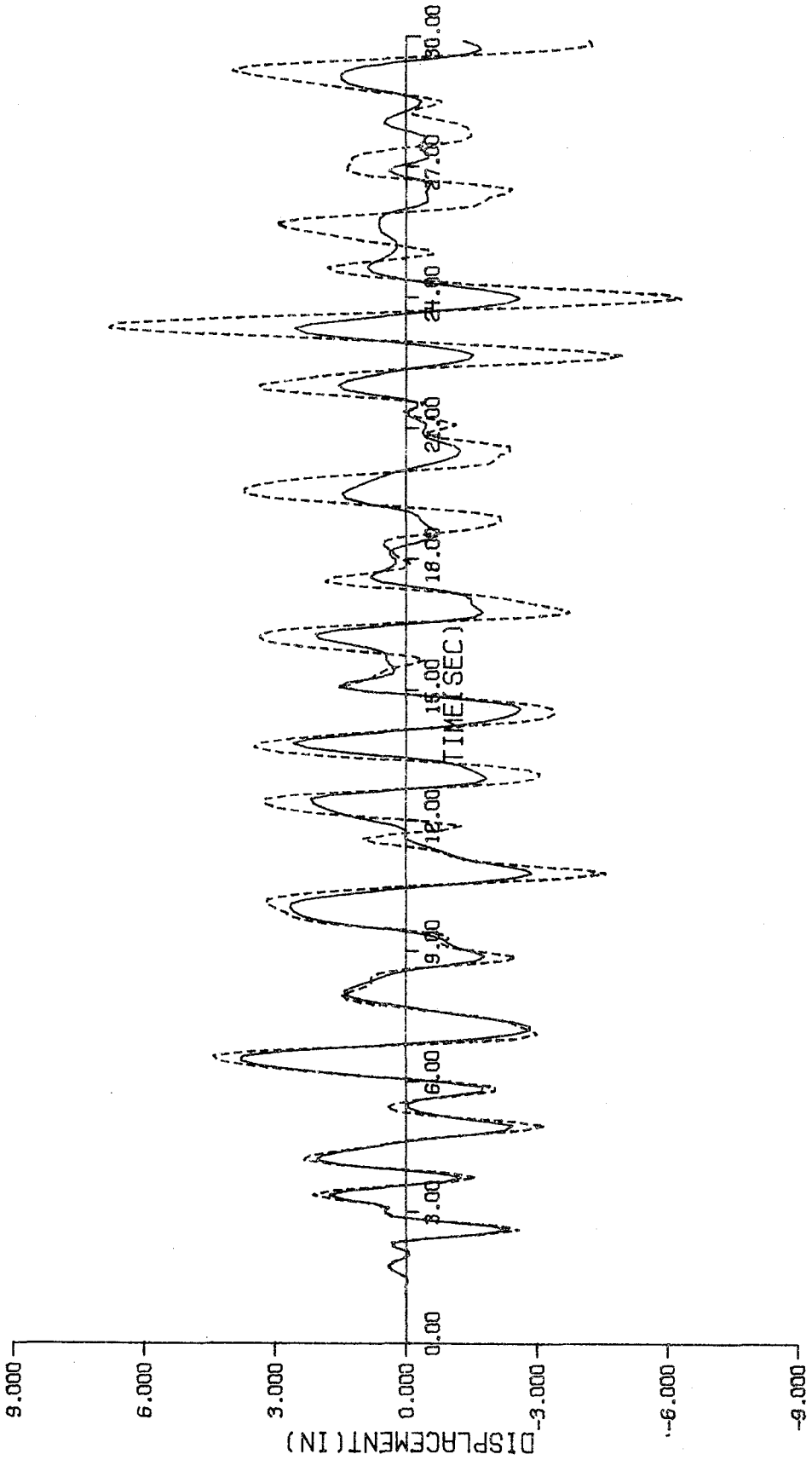

Fig. 14 Time history of the y-displacement at Point C for the frame-fixed case.
---- undamped; ____ 1.5% damping.

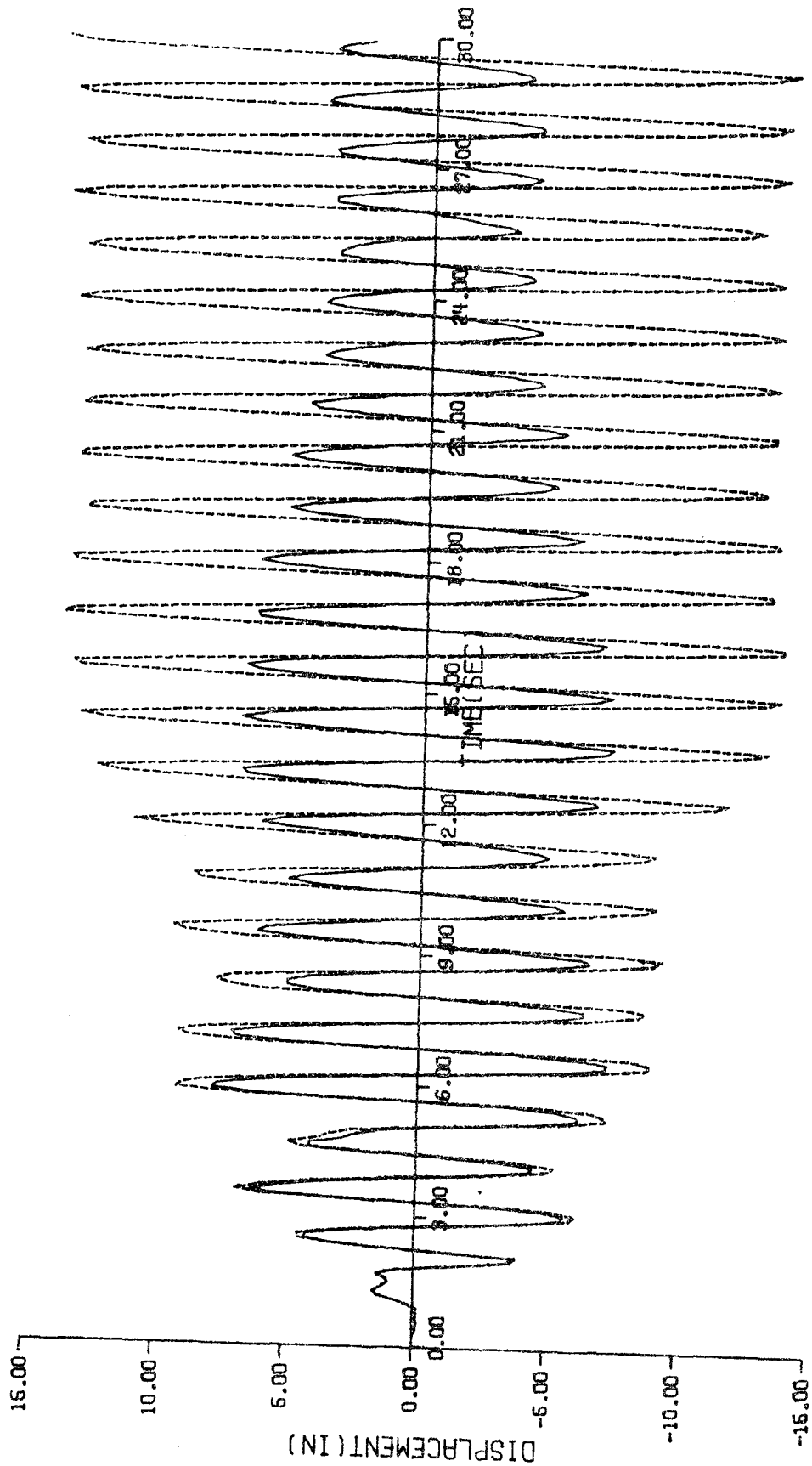

Fig. 15 Displacement in x-direction at the upper end of the pipe for the frame-fixed case.
——— 1.5% damping; ---- undamped.

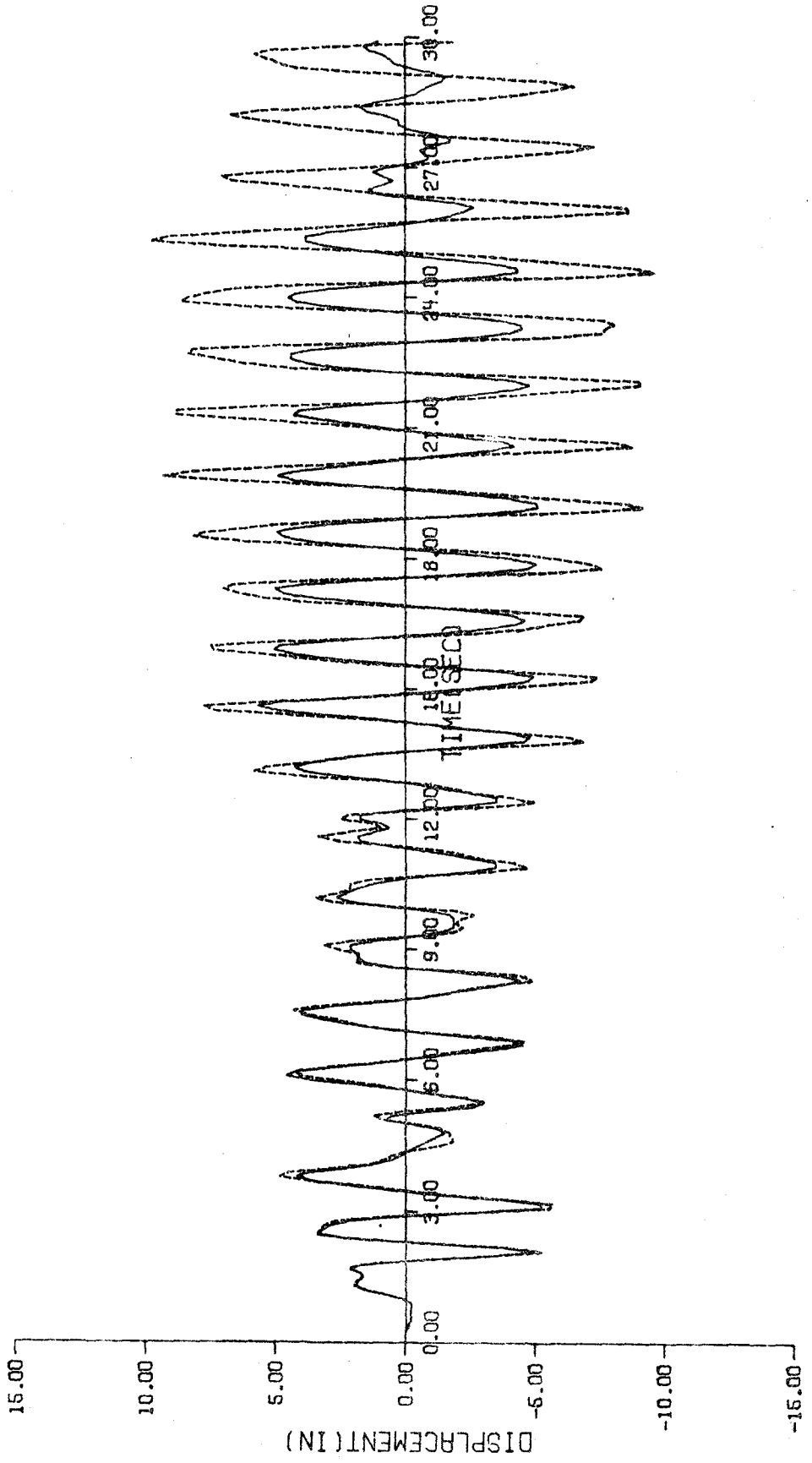

Fig. 16 Displacement in y-direction at the upper end of the pipe for the frame-fixed case.
——— 1.5% damping; --- undamped.

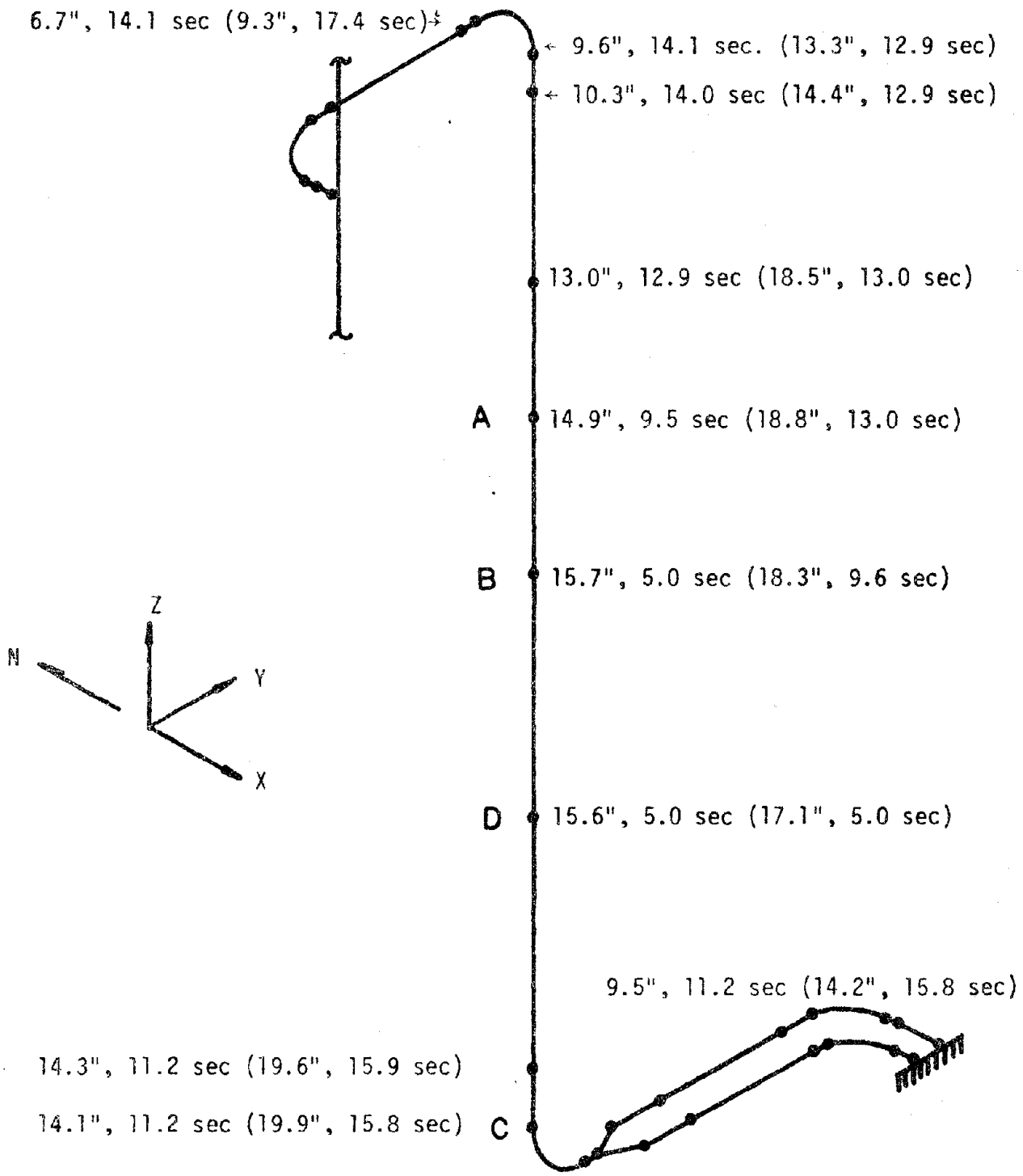

Fig. 17 Maximum 1.5% - damped (undamped) x-displacements and times (seconds) of occurence for the fixed-fixed case.

18, respectively. Quantities in the parentheses are results for the undamped case.

The time histories of the bending moments and torque at Point C are presented in Figs. 19-24. In these figures, solid lines are solutions for 1.5 percent damping and dashed lines are solutions for zero damping. The bending moments Mx and My and the torque for the fixed-fixed system are shown in Figs. 19, 20 and 21, respectively. The corresponding solutions for the frame-fixed system are presented in Figs. 22-24. It is found that the amplitudes of the moment and torque are larger in the frame-fixed system than those in the fixed-fixed system. For the bending moments, they exhibit more oscillatory behavior in the fixed-fixed system than in the frame-fixed system. However, opposite behavior in the torque is observed.

Figures 25-28 depict the instantaneous deformed configurations in the fixed-fixed system at times when the x-displacement at Point C becomes substantially large. Both 1.5 percent damping and zero damping are considered. Similar instantaneous deformed configurations in the frame-fixed system are presented in Figs. 29-32. It is interesting to note that the deformed configurations in the fixed-fixed case resemble that of the lowest mode in free vibration. While for the frame-fixed case, the transient deflection looks similar to the fifth mode in free vibration. This indicates that during an earthquake, the motion of the system could be dominated by a single mode.

It is well known that natural frequency is proportional to the square root of the stiffness of a structure. Thus, if the Young's modulus $E = 20 \times 10^6$ psi is used instead of $E = 23 \times 10^6$ psi for the pipe, little change in the natural frequency is expected. However, it is observed that

a relatively small change in the Young's modulus causes a rather significant change in the transient response of the system as depicted in Fig. 33. The difference becomes more pronounced as time passes. This might be caused by a greater participation of higher modes in the transient vibraton when the stiffness of the system is lowered.

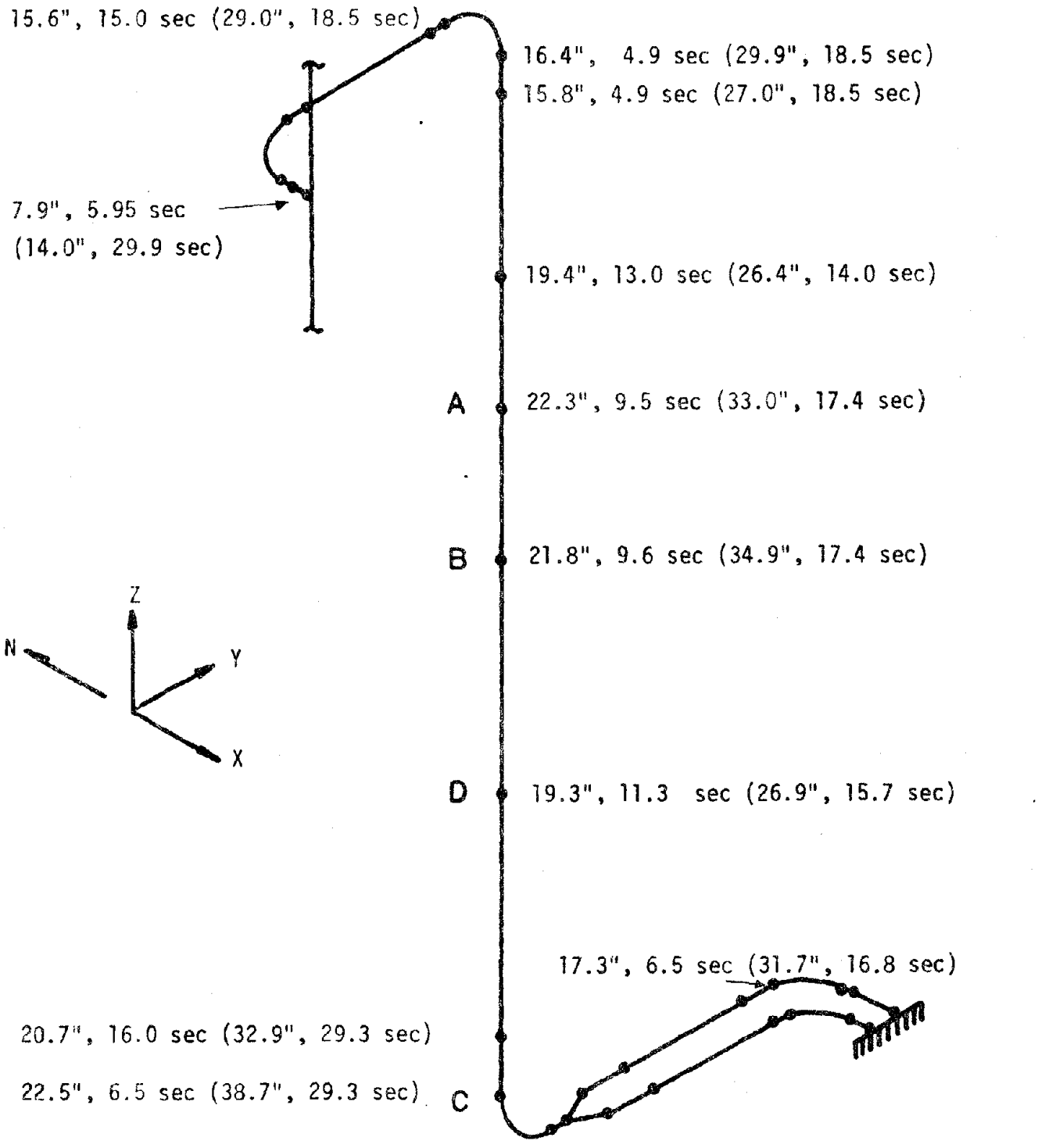

Fig. 18 Maximum 1.5% - damped (undamped) x-displacements and times (seconds) of occurence for the frame-fixed case.

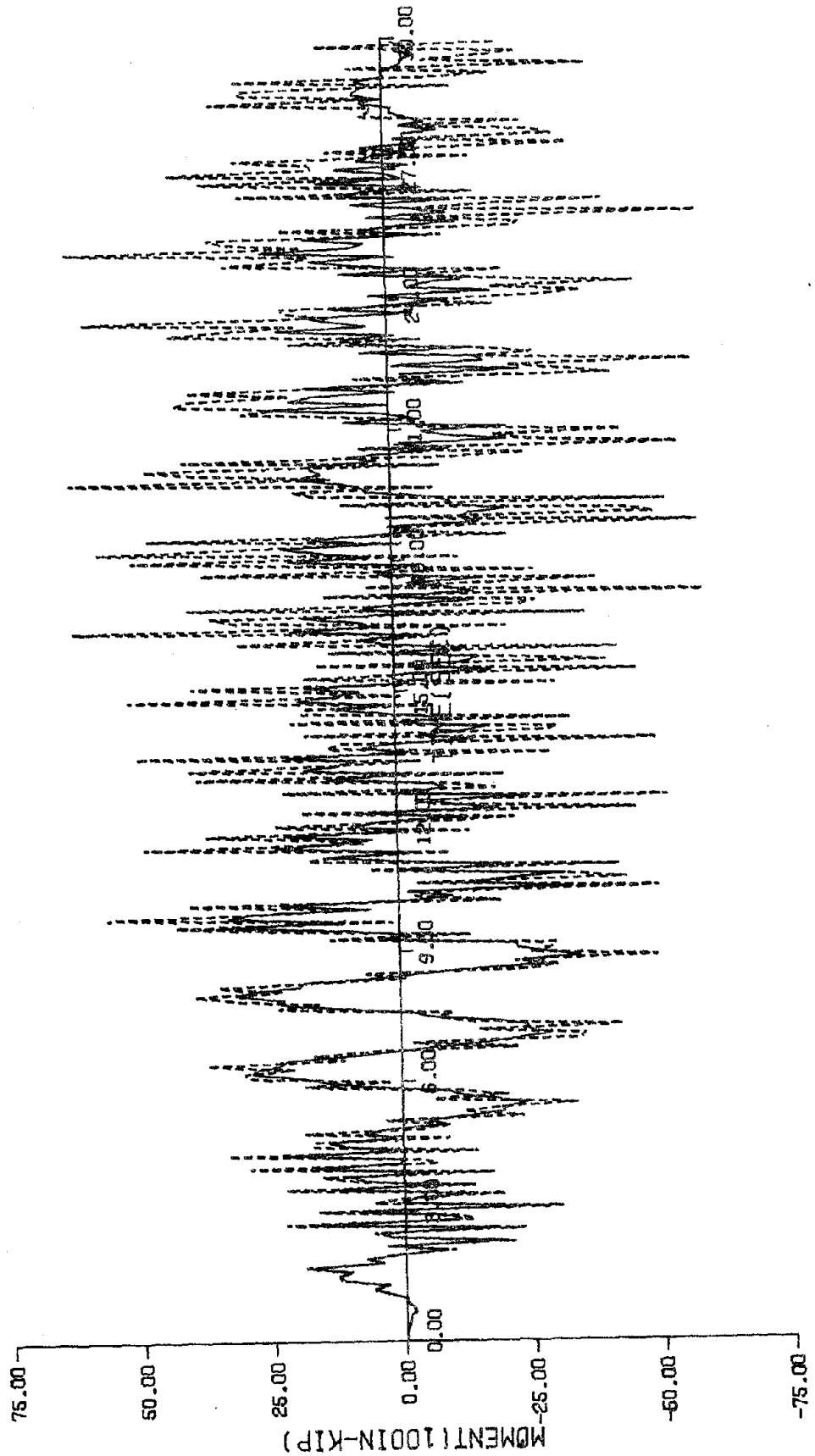

Fig. 19 Time history of the bending moment Mx at Point C in the fixed-fixed system.
——— 1.5% damping; ---- undamped.

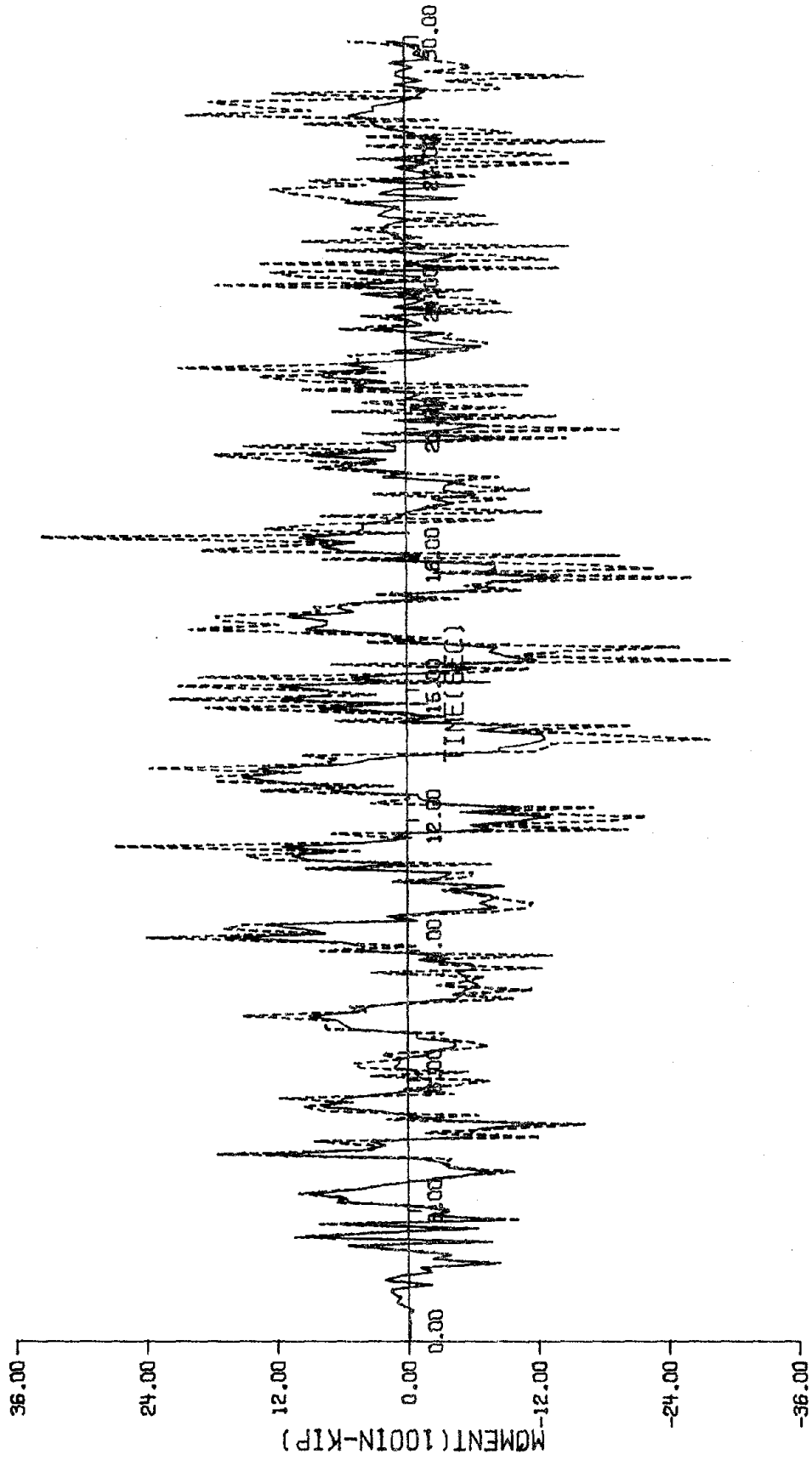

Fig. 20 Time history of the bending moment My at Point C in the fixed-fixed system.
——— 1.5% damping; ---- undamped.

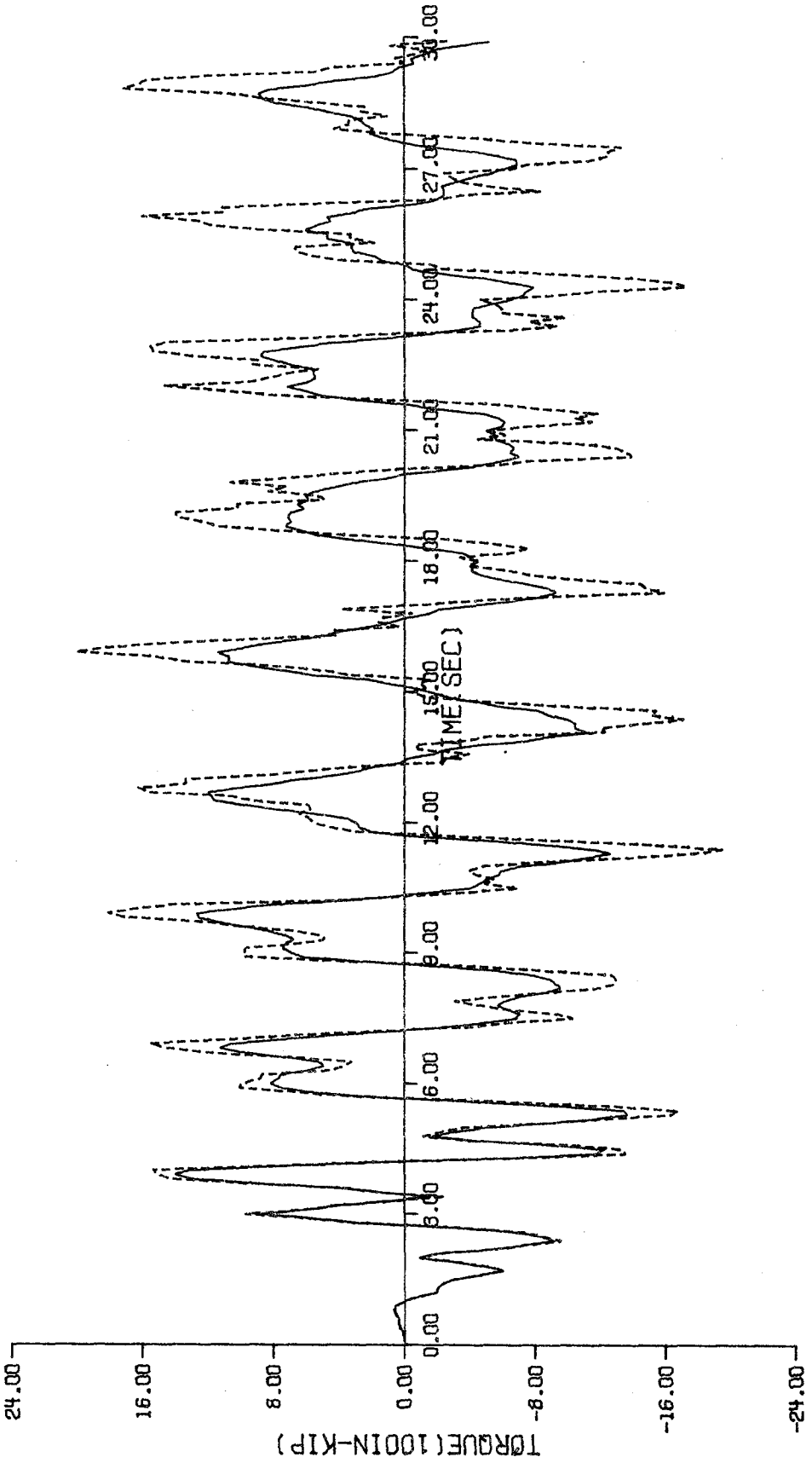

Fig. 21 Time history of the torque T at Point C in the fixed-fixed system.
____ 1.5% damping; ---- undamped.

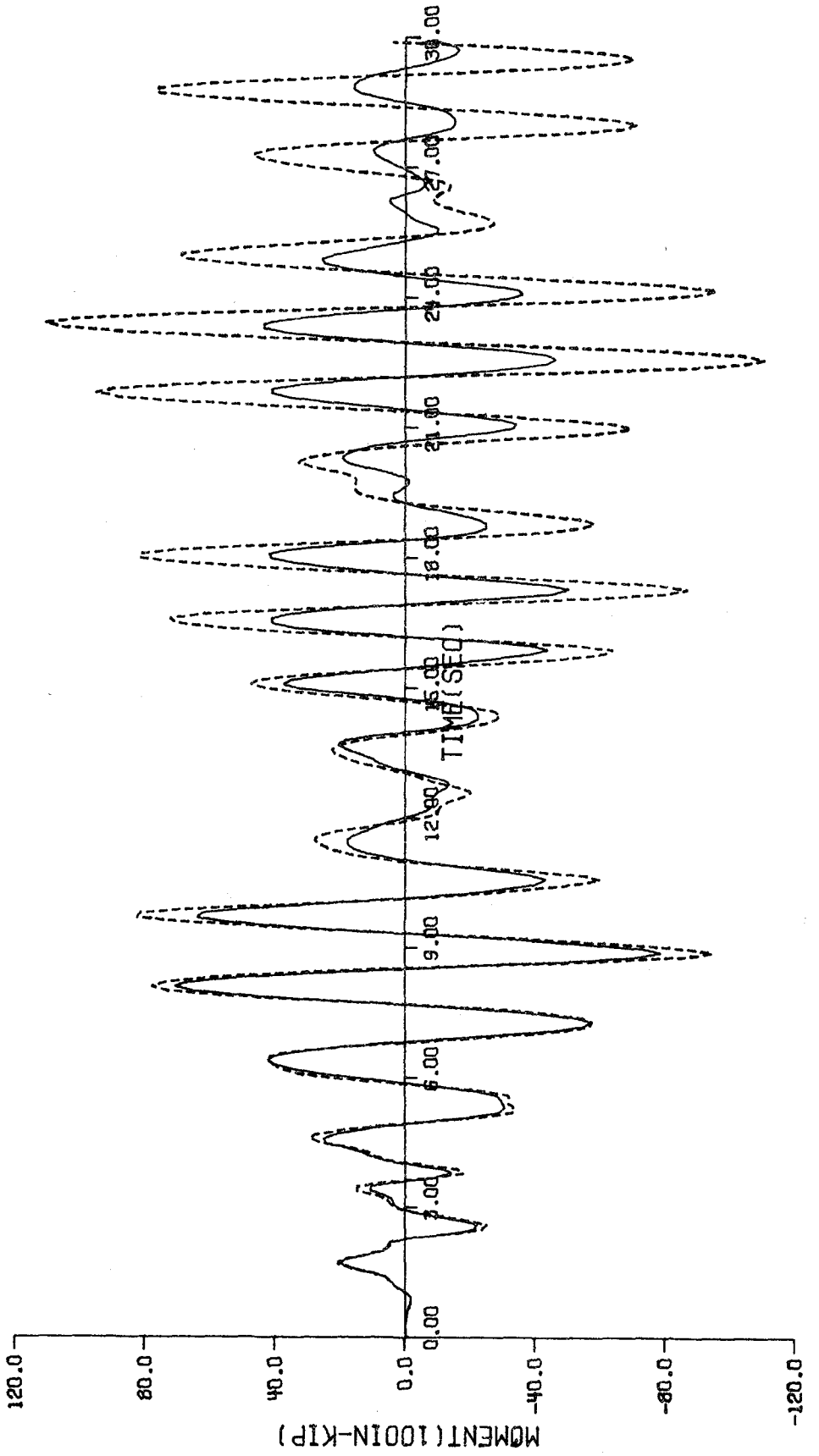

Fig. 22 Time history of the bending moment Mx at Point C in the frame-fixed system. ____ 1.5% damping; ---- undamped.

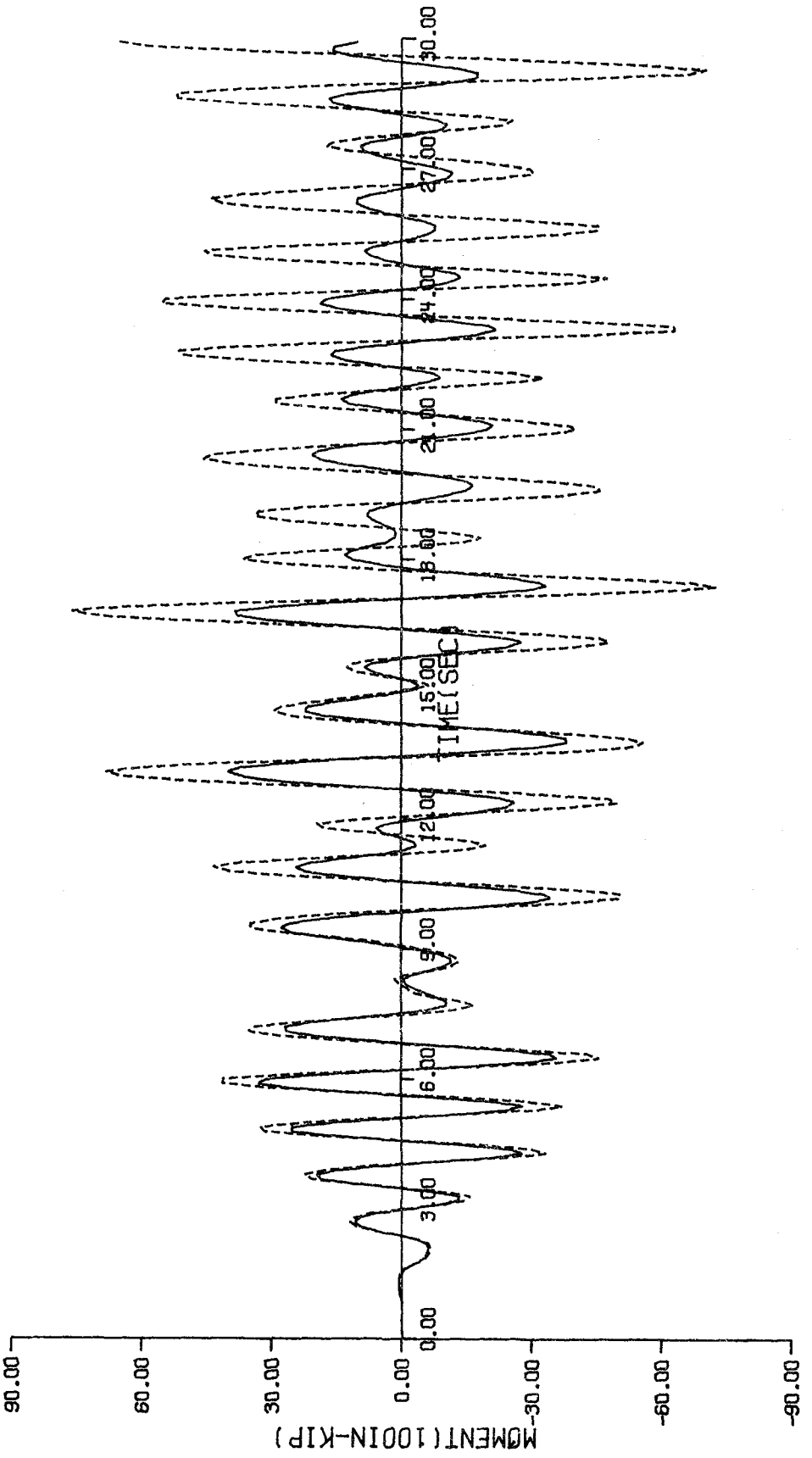

Fig. 23 Time history of the bending moment My at Point C in the frame-fixed system. ____ 1.5% damping; ---- undamped.

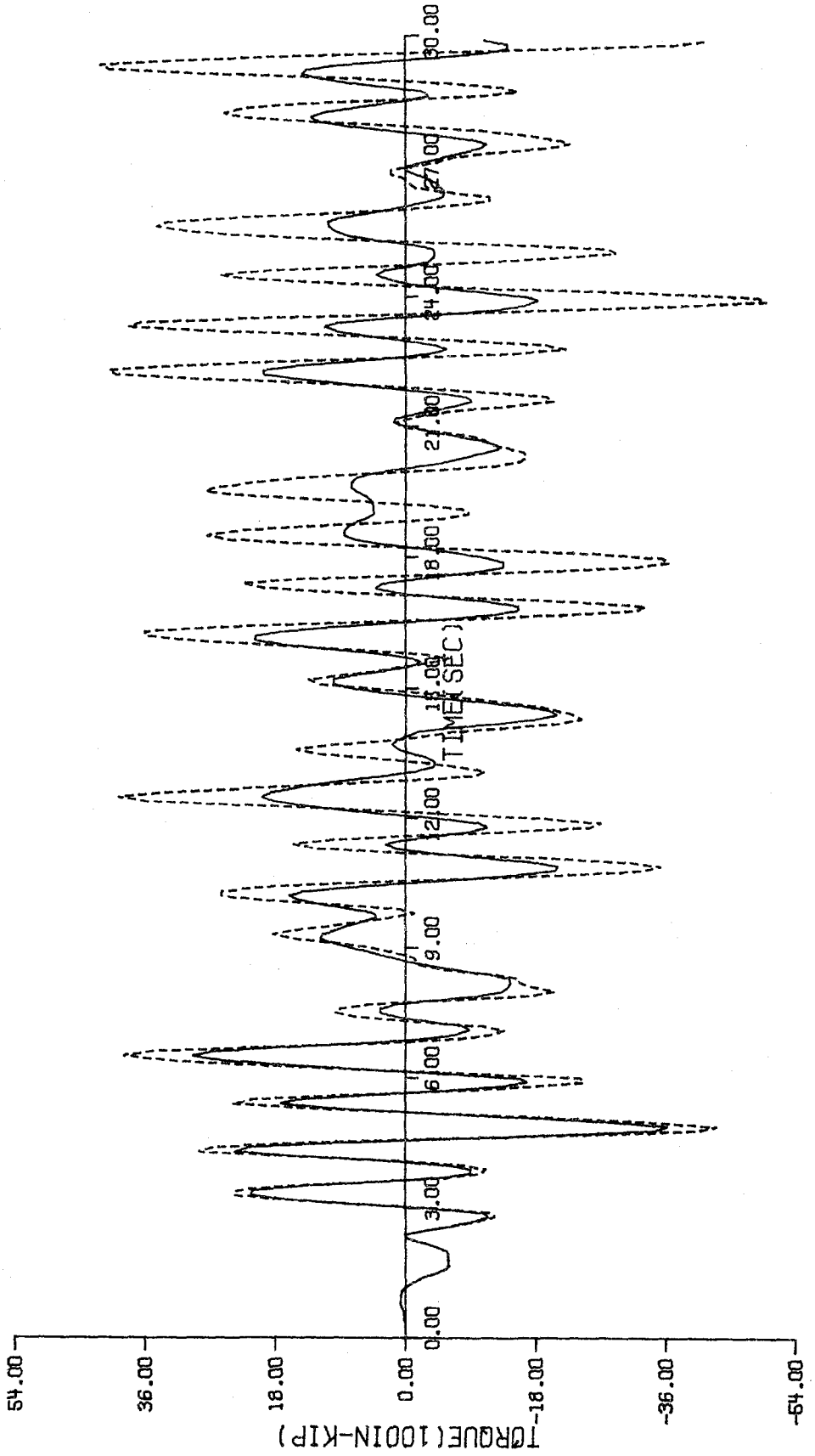

Fig. 24 Time history of the torque T at Point C in the frame-fixed system. ____ 1.5% damping; ---- undamped.

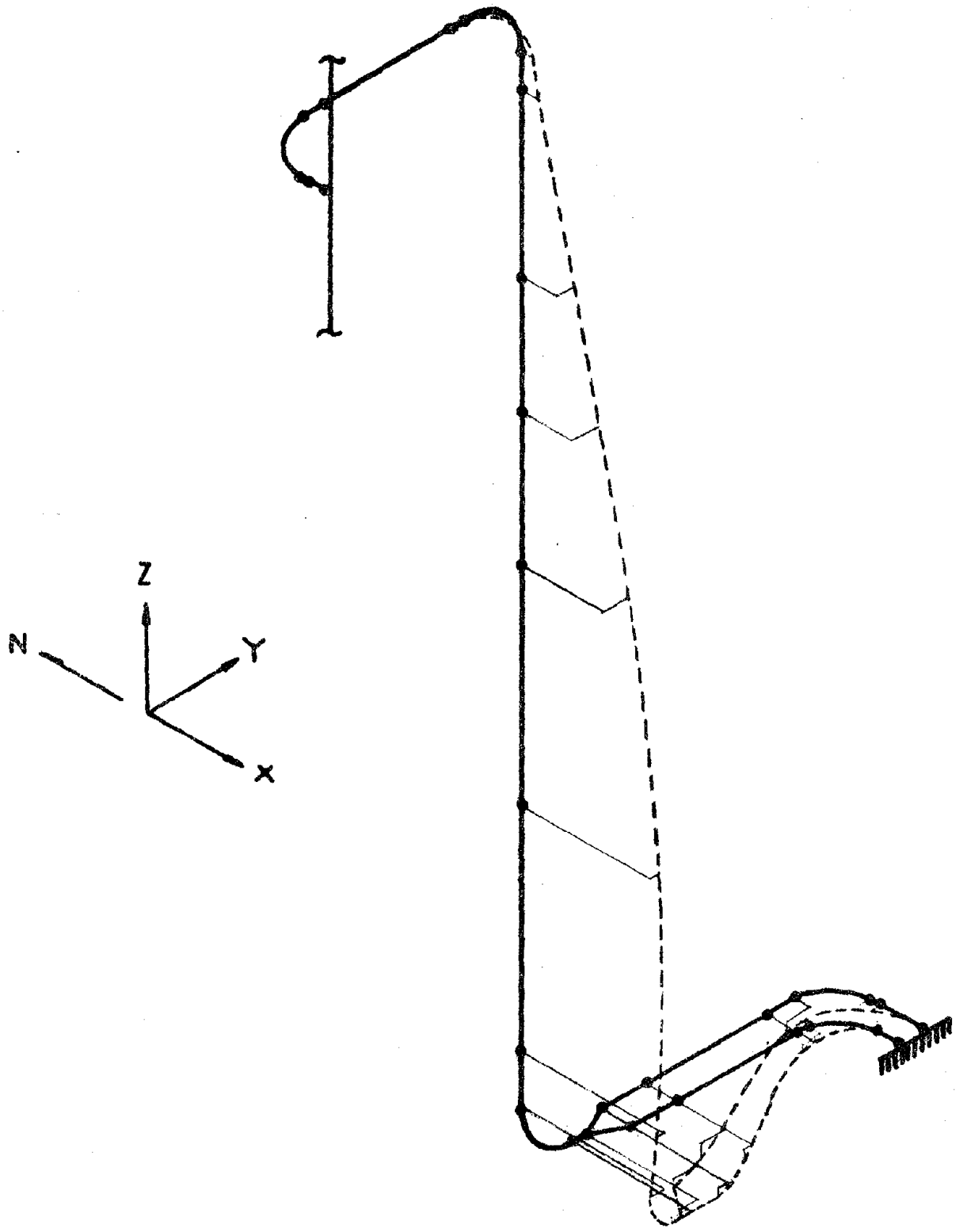

Fig. 25 Deformed configuration of pipe at t = 11.3 sec for the fixed-fixed case with 0 damping

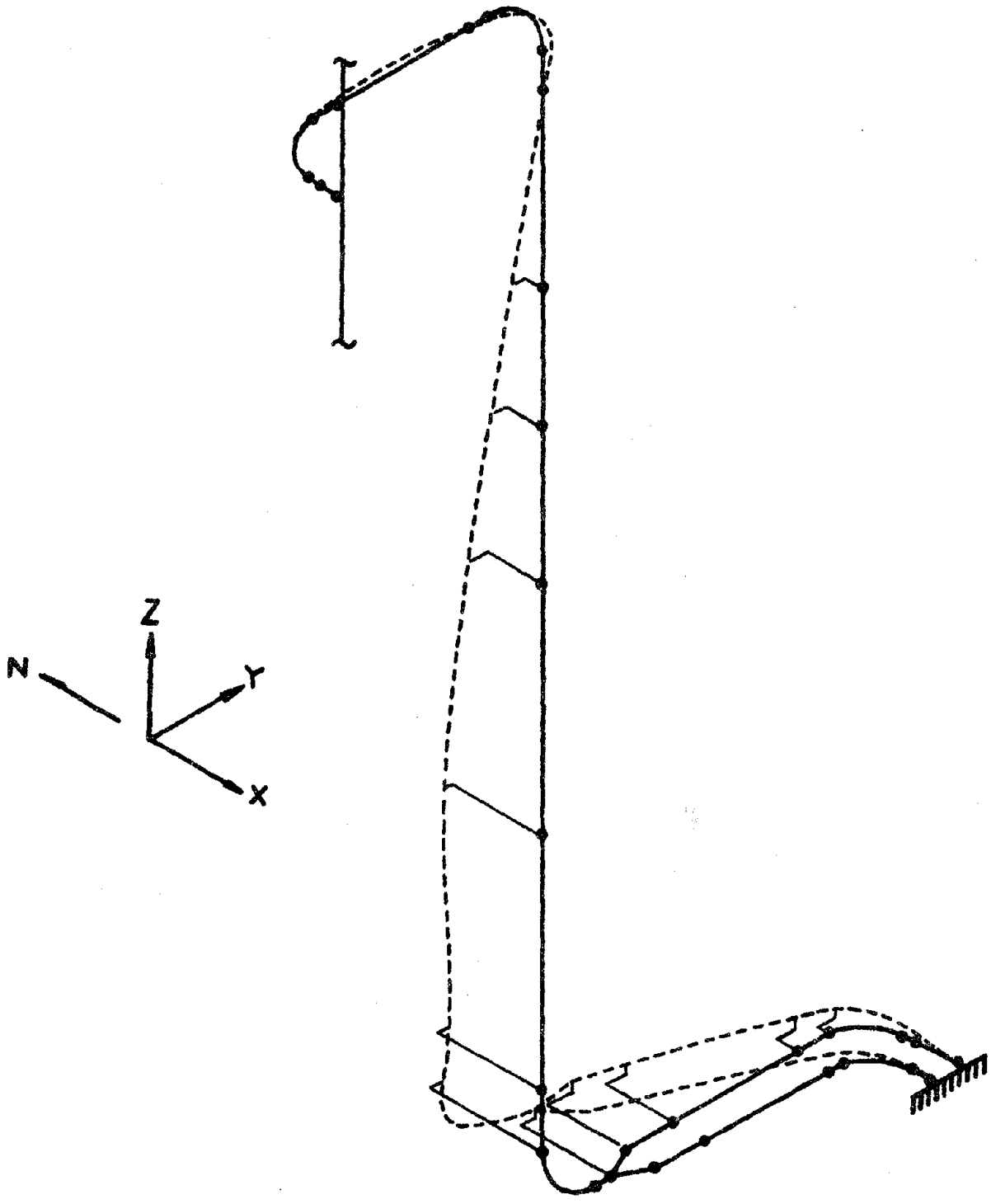

Fig. 26 Deformed configuration of pipe at t = 15.8 sec for the fixed-fixed case with 0 damping

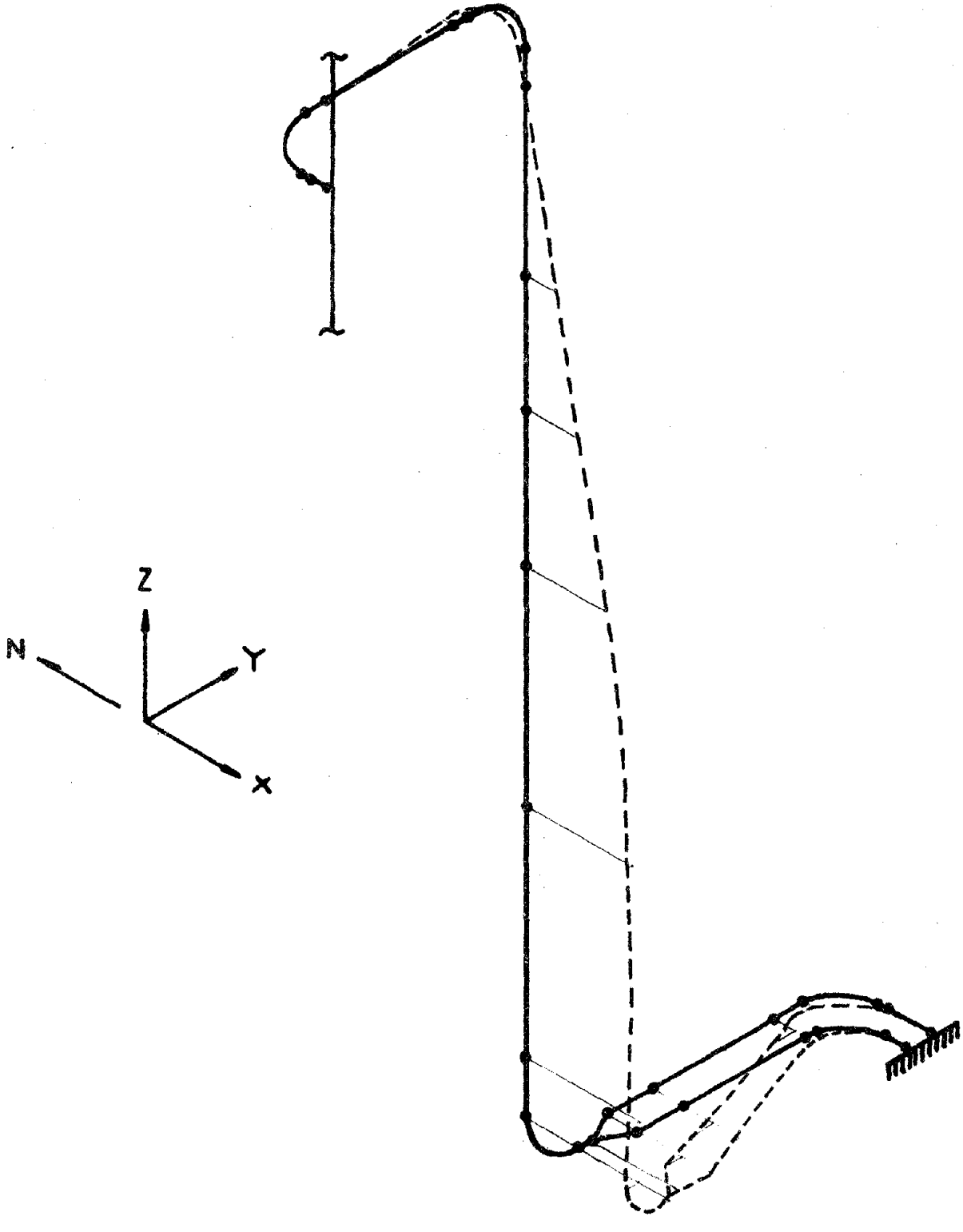

Fig. 27 Deformed configuration of pipe at t = 11.2 sec for the fixed-fixed case with 1.5% damping

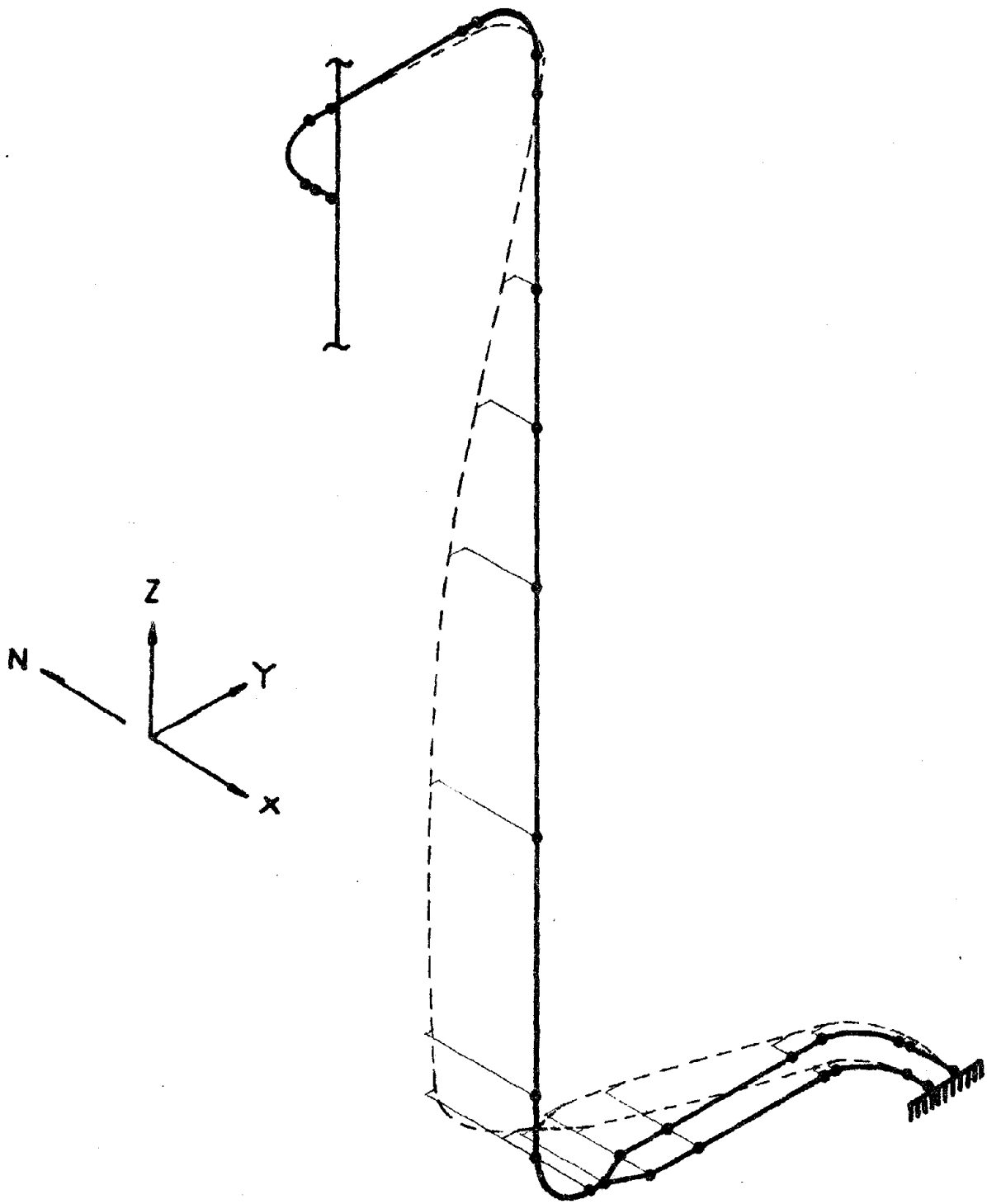

Fig. 28 Deformed configuration of pipe at t = 15.8 sec for the fixed-fixed case with 1.5% damping

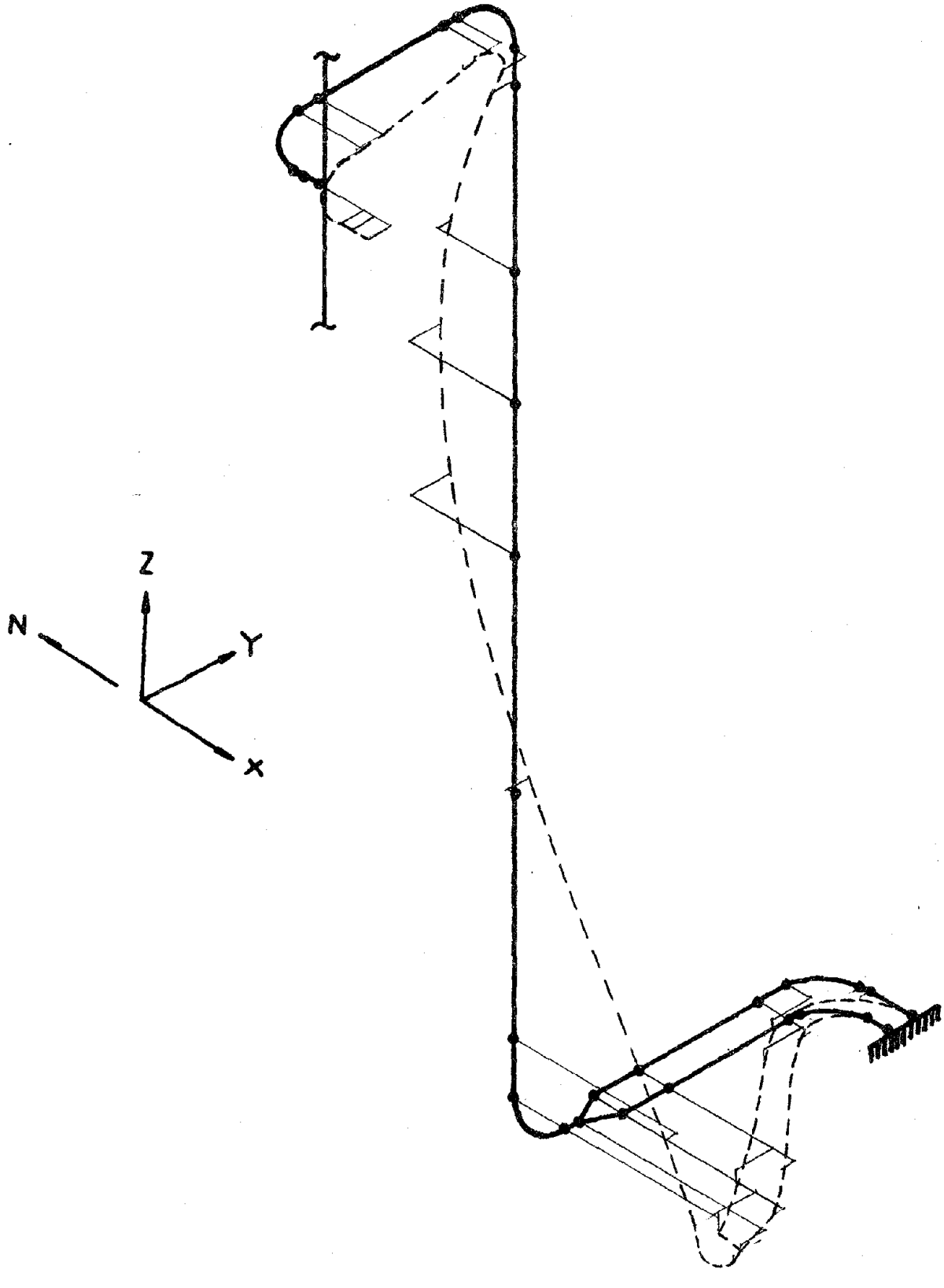

Fig. 29 Deformed configuration of pipe at t = 16.8 sec for the frame-fixed case with 0 damping

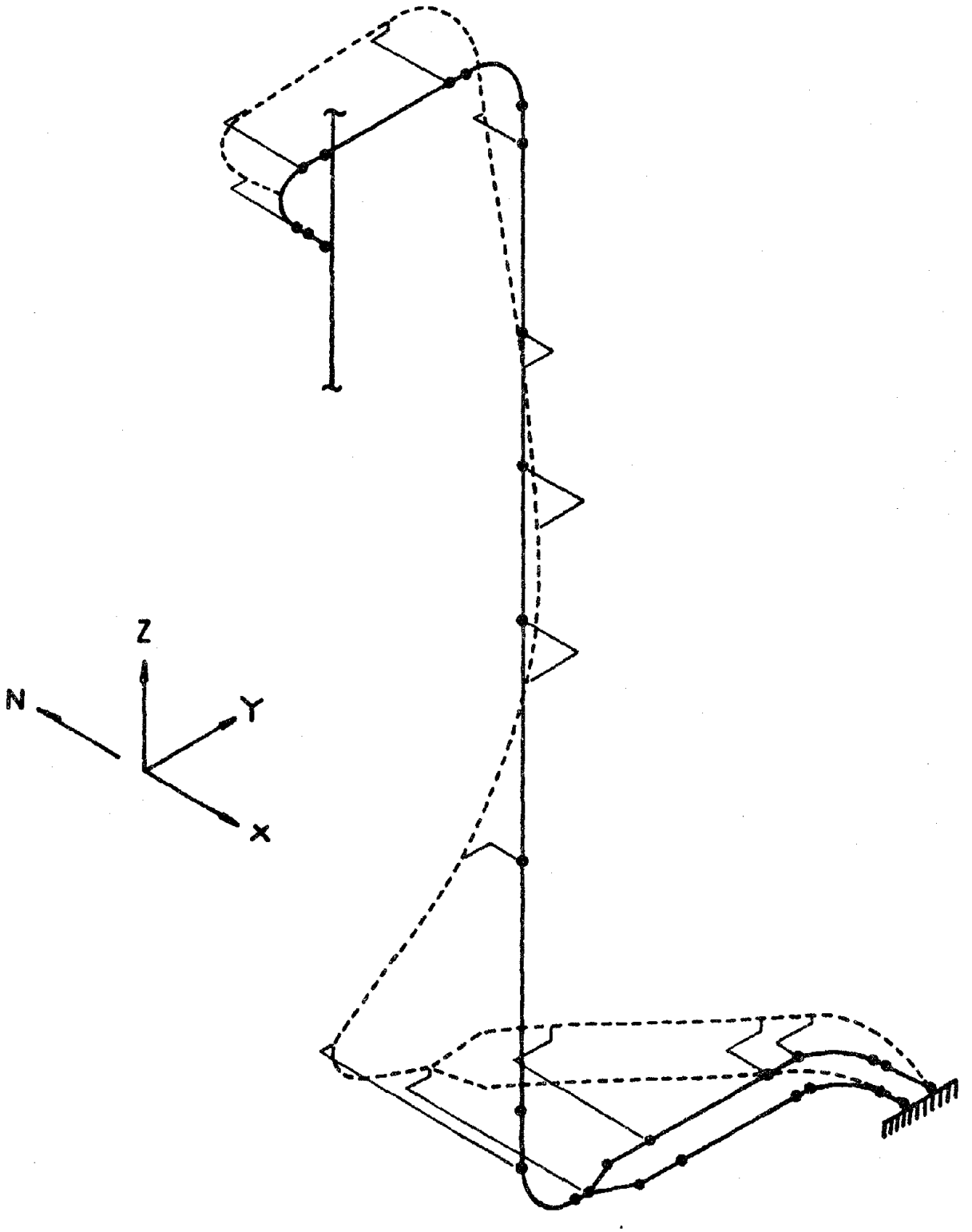

Fig. 30 Deformed configuration of pipe at t = 29.3 sec for the frame-fixed case with 0 damping

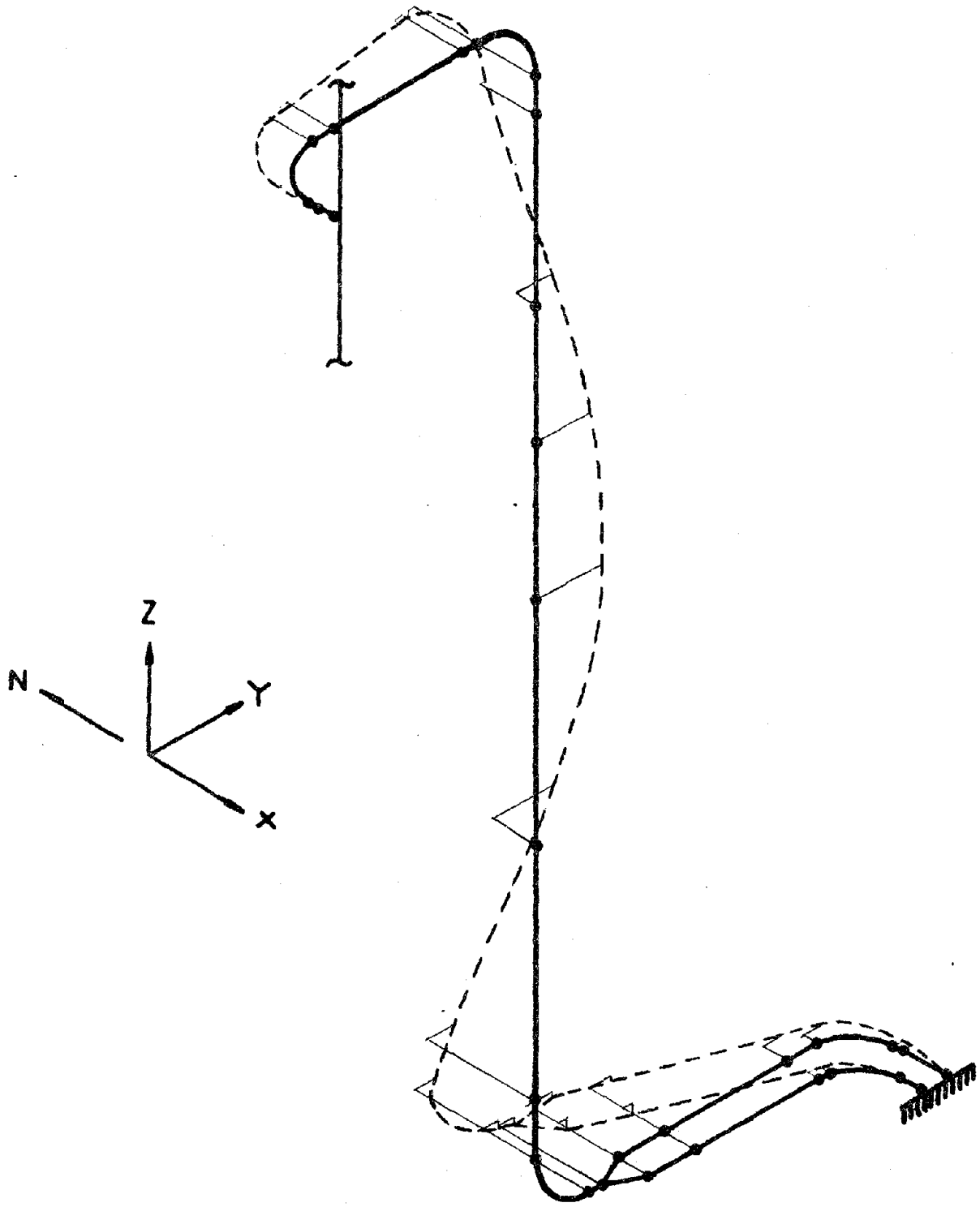

Fig. 31 Deformed configuration of pipe at t = 6.5 sec for the frame-fixed case with 1.5% damping

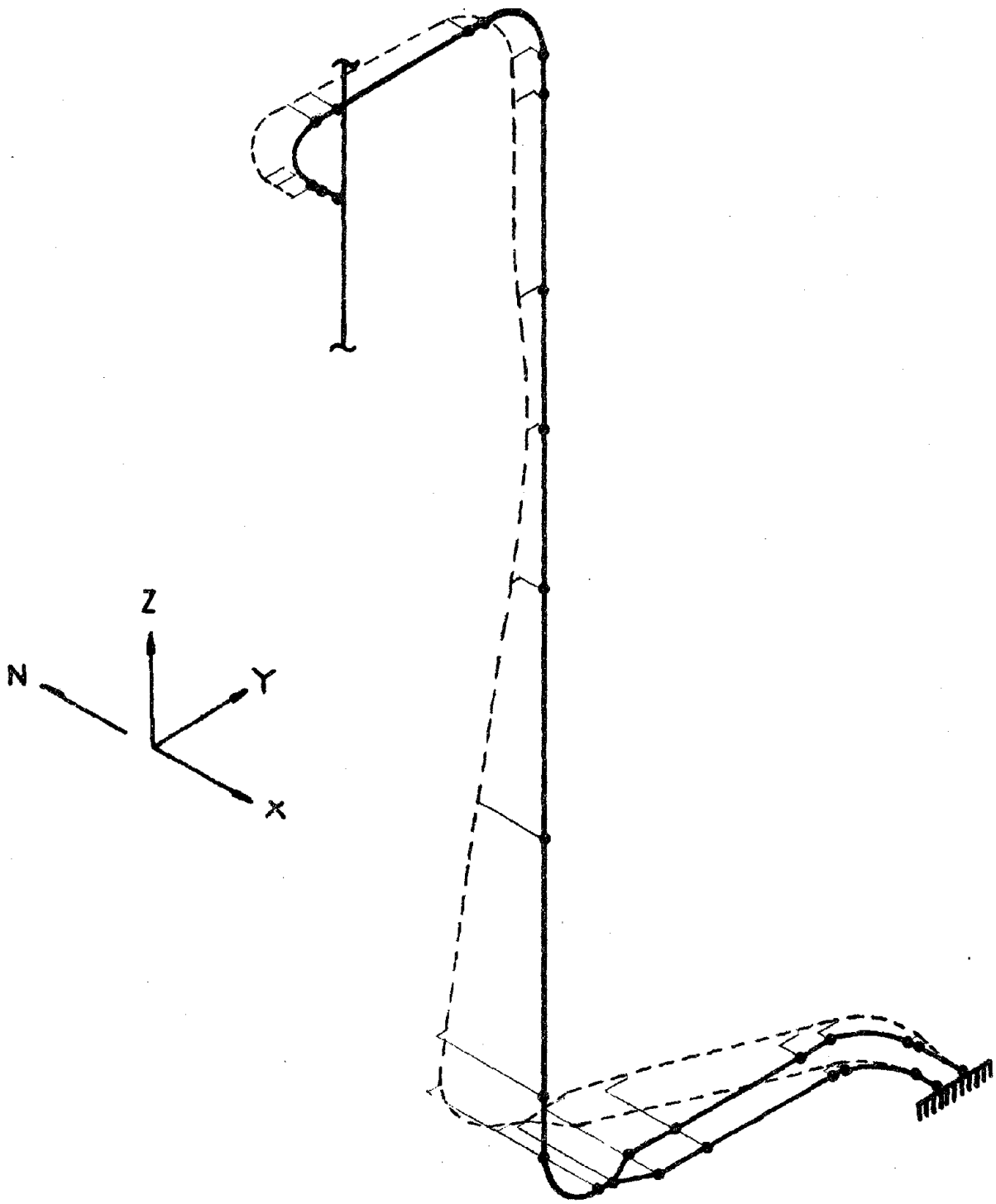

Fig. 32 Deformed configuration of pipe at t = 12.4 sec for the frame-fixed case with 1.5% damping

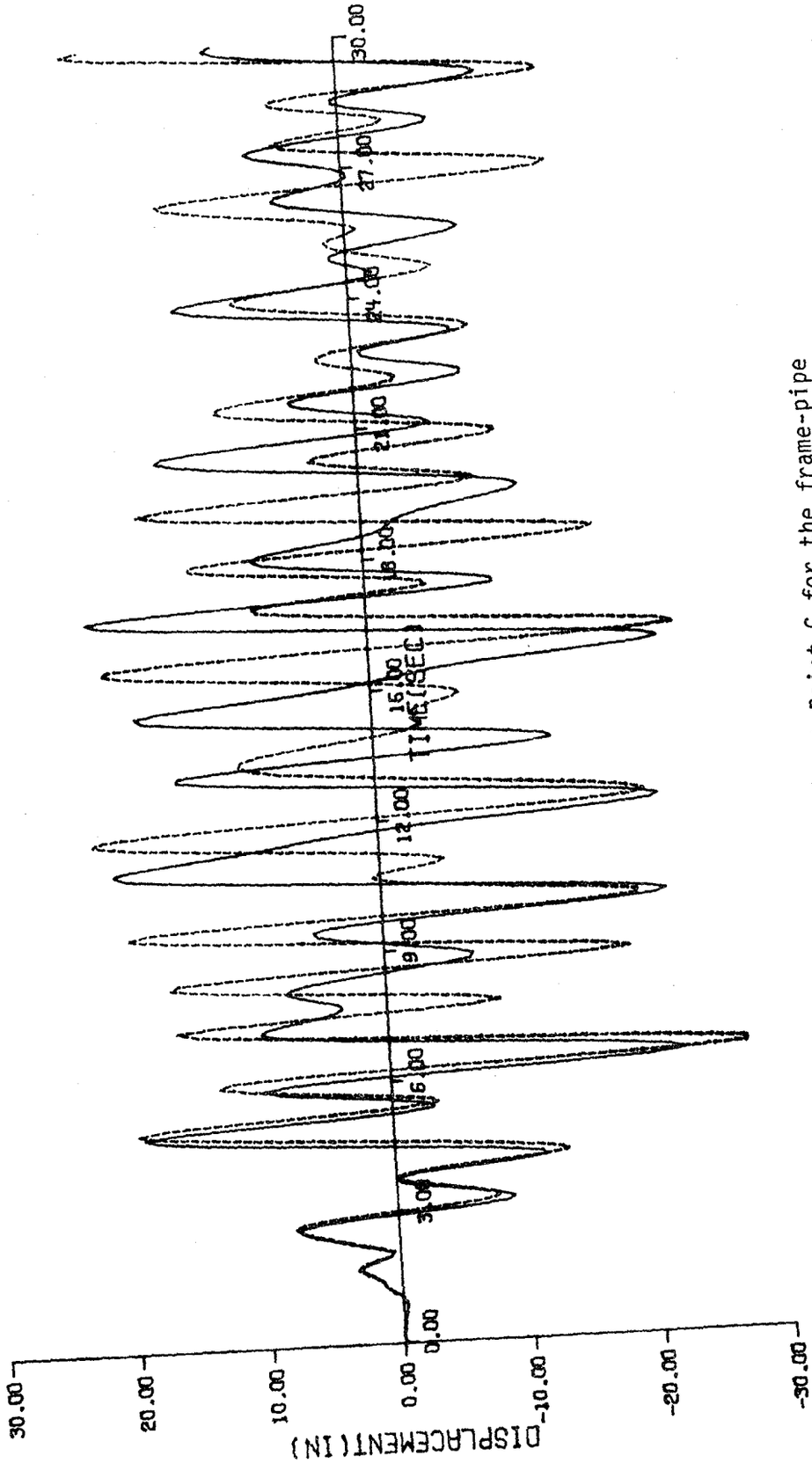

Fig. 33 Displacement in the x-direction at Point C for the frame-pipe system. ——— E = 23 x 10⁶ psi; ---- E = 20 x 10⁶ psi. 1.5% damping is assumed.

STRESS ANALYSIS

Of major importance is to know if the piping system can withstand the seismic load. For this consideration, we take the worst conditions that take place during the entire history of response of the pipe. The maximum combined stress is obtained from

$$\sigma = \frac{16 d_o}{\pi(d_o^4 - d_i^4)} (M + \sqrt{M^2 + T^2}) \qquad (2)$$

where d_o is the outer diameter of the pipe, d_i is the inner diameter, T is the torque and

$$M = \sqrt{M_x^2 + M_y^2} \qquad (3)$$

is the maximum combined bending moment. In Eq. (3), M_x and M_y are the bending moments.

The maximum bending moments, torques, and times of occurence are presented in Figs. 34 and 35 for the fixed-fixed and frame-pipe systems, respectively. The results are obtained using 1.5 percent damping. From Fig. 34, it appears that the most critical place is at Point D for the fixed-fixed system. The maximum bending moments and torque are

$$M_x = 7.58 \times 10^6 \text{ in-lb at } 4.9 \text{ sec}$$
$$M_y = 3.64 \times 10^6 \text{ in-lb at } 9.6 \text{ sec}$$
$$T = 1.40 \times 10^6 \text{ in-lb at } 3.9 \text{ sec} \qquad (4)$$

The maximum principal stress according to Eq. (2) is obtained as

$$\sigma = 10{,}600 \text{ psi} \qquad (5)$$

Note that in the foregoing calculation, the maximum moments about the x-axis and y-axis do not occur at the same time. This estimate is thus very conservative.

For the frame-pipe system, the most critical place seems to be at Point B. The maximum bending moments, torque, and times of occurence are

$$M_x = 14.9 \times 10^6 \text{ in-lb at } 5.4 \text{ sec}$$

$$M_y = 10.9 \times 10^6 \text{ in-lb at } 8.9 \text{ sec}$$

$$T = 3.63 \times 10^6 \text{ in-lb at } 4.9 \text{ sec} \qquad (6)$$

The maximum principal stress is

$$\sigma = 23{,}300 \text{ psi} \qquad (7)$$

It is evident that in both cases, the maximum principal stresses are below the yield strength (28000 psi) of the material.

Although from the yield consideration this piping system seems to be safe in the earthquake, the large swing of certain portion of the pipe might cause collisions of the pipe against the surrounding structures. Failure due to such collision should not be overlooked.

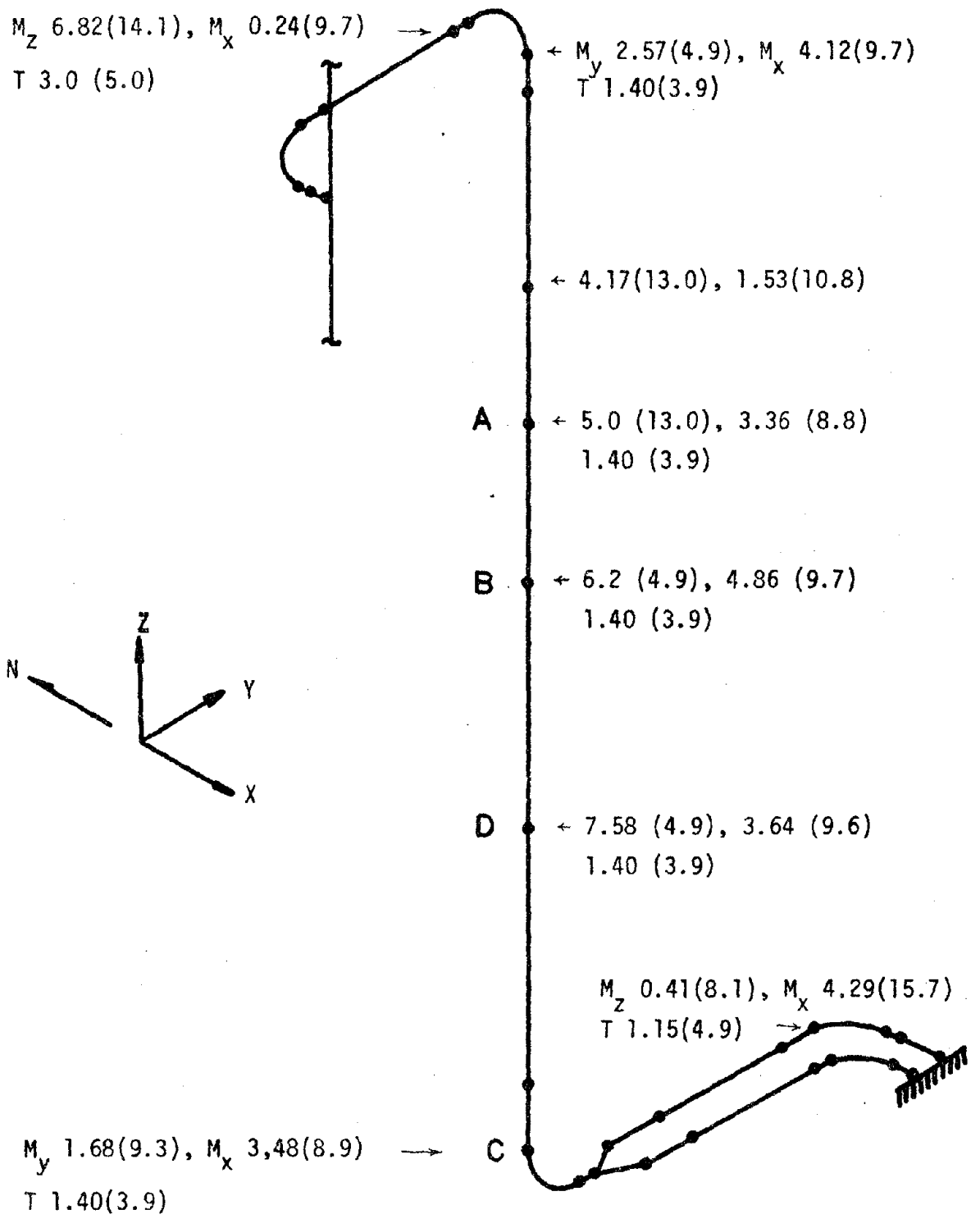

Fig. 34 Maximum 1.5% - damped bending moments and torque(10^6 in-lb) and times (seconds) of occurence for the fixed-fixed case. The times of occurence are placed in parentheses.

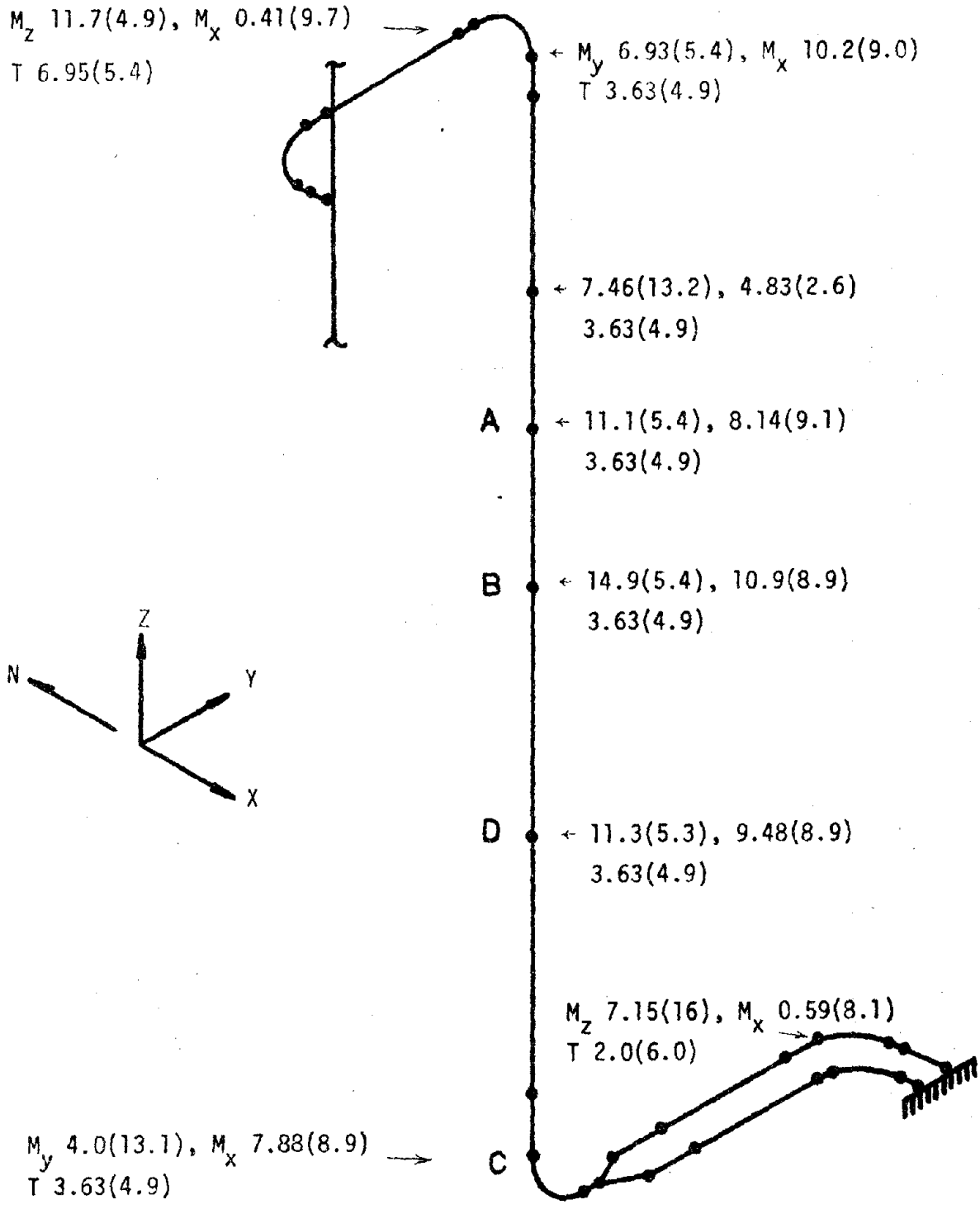

Fig. 35 Maximum 1.5% - damped bending moments and torque (10^6 in-lb) and times (seconds) of occurence for the frame-fixed case. The times of occurence are placed in parentheses.

ACKNOWLEDGEMENTS

This work was supported by the National Science Foundation under Grant No. GI4-1897 to Purdue University. The authors wish to thank A.S. Ledger, A. Rois-Mendez, and C.C. Chen for their assistance in numerical computations. Valuable comments from members of the Advisory Committee are also acknowledged.

REFERENCES

1. Shibata, H., Watari, A., Fujii, S., Iguchi, J., Sato, H., and Shigeta, T., "Aseismic Design of Piping Systems in Power and Chemical Engineering Plants," Proceedings of Japanese Society of Mechanical Engineers 1967 Semi-International Symposium, Tokyo, September 1967, pp. 215-222.

2. Shimizu, N., and Shibata, H., "Response Analysis of Piping Systems to Multi-Inputs," Bulletin of the Japanese Society of Mechanical Engineers, Vol. 15, No. 81, 1972, pp. 307-315.

3. Chen, L.H., "Piping Flexibility Analysis by Stiffness Matrix," Journal of Applied Mechanics, Vol. 26, 1959, pp. 608-612.

4. Lin, C.W., "Seismic Analysis of Piping Systems," Nuclear Engineering and Design, Vol. 11, 1970, pp. 217-224.

5. Chen, C.C., Sun, C.T., Bogdanoff, J.L., and Lo, H., "Simple Models for Computing Dynamic Response of Complex Frame Structures," To be published.

6. Yang, T.Y., Baig, M.I., and Bogdanoff, J.L., "Dynamic Behavior of the Steam Generator and Support Structures of the 1200 MW Fossil Fuel Plant Unit #3, Paradise, Kentucky," technical report to be submitted to National Science Foundation.